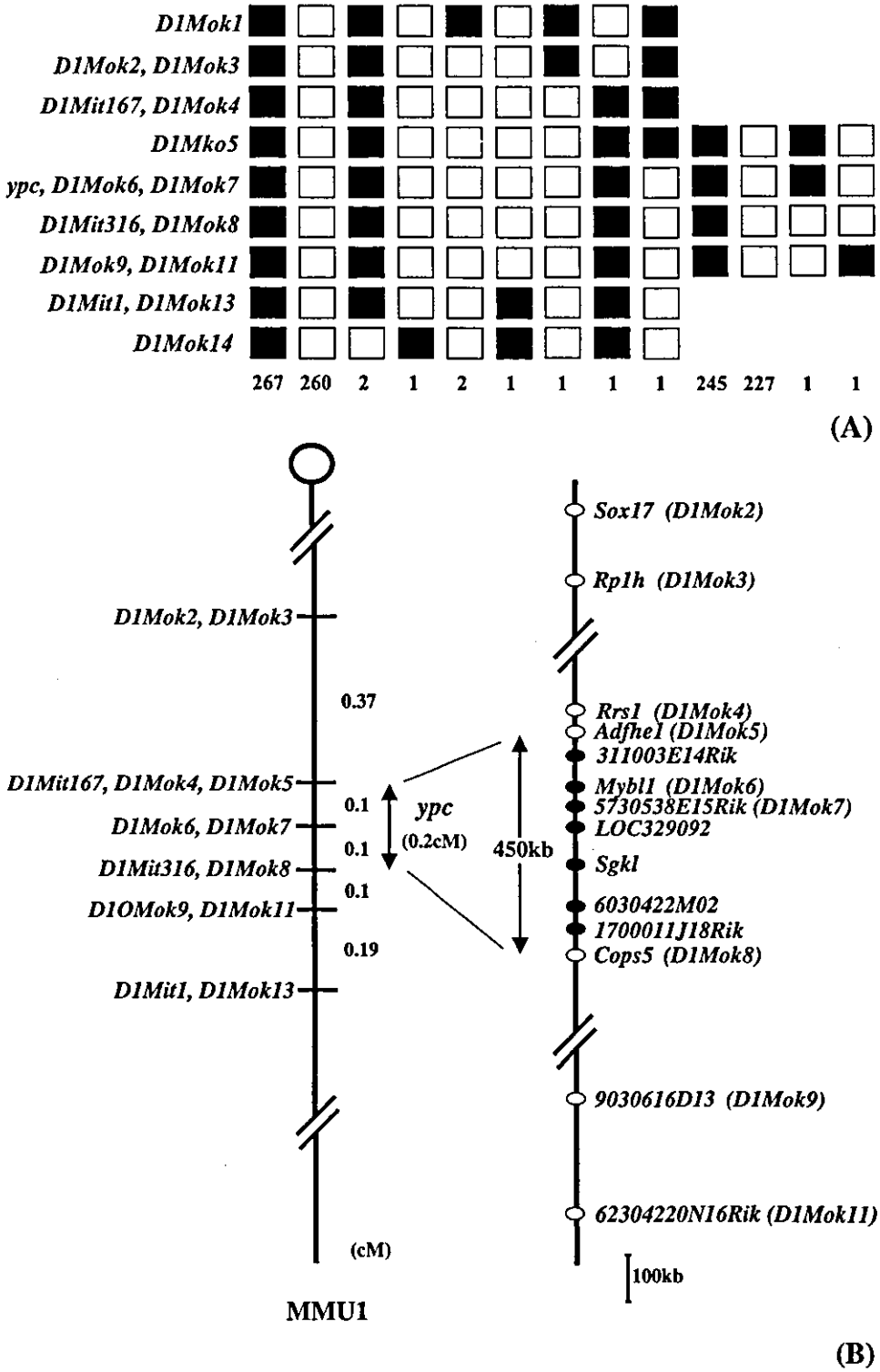

Figure 3. Localization of the *ypc* locus on mouse chromosome 1. (A) Segregation of haplotypes in 1010 backcross mice obtained from crosses between YPC and JF1/Msf strains. Open and filled boxes represent homozygosity of the YPC type alleles and heterozygous F_1 type, respectively. The genotypes of the *ypc* locus (*ypc/ypc* or *ypc/+*) are also denoted by the open and filled boxes. The number of backcross mice for each haplotype is indicated at the bottom of each column. (B) A partial linkage map of mouse chromosome 1 obtained in the present study and corresponding physical map obtained from the mouse genome sequence. Location of the *ypc* locus in relation to the linked loci is shown by an arrow. Positions of the genes, ESTs, and predicted genes are shown in the physical map with their related microsatellite markers. Distances are shown in cM and in kb on the linkage and physical maps, respectively.

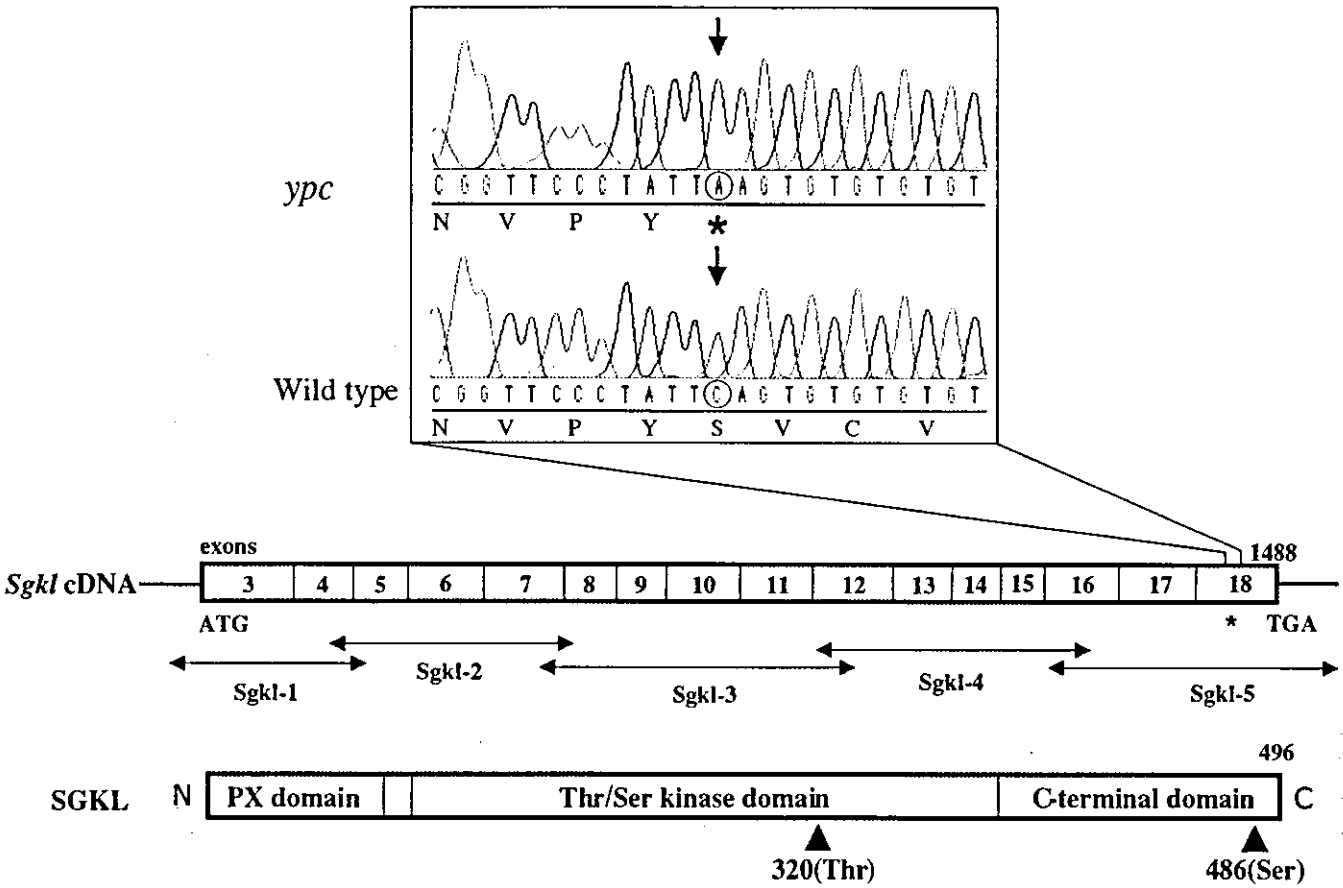

Figure 4. Chromatograms showing a nucleotide substitution in the *Sgkl* gene and structure of *Sgkl* cDNA and SGKL. Horizontal arrows indicate the amplified fragments which cover the entire coding region of the gene. Vertical arrows in the chromatograms indicate the C-to-A nucleotide substitution at codon 461. The serine and threonine residues (Ser486 and Thr320) that are phosphorylated in response to signals from PI3K are indicated by arrowheads. Asterisks indicate the premature termination codon.

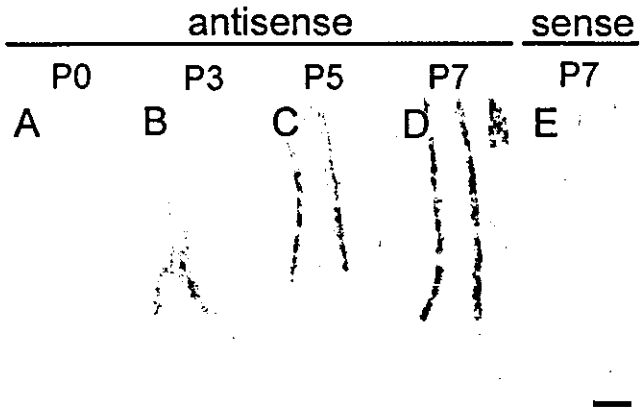

Figure 5. Expression of *Sgkl* mRNA in developing hair follicles. A to D: *In situ* hybridization with *Sgkl* antisense probe. E: *In situ* hybridization with *Sgkl* sense probe. At P0, no signal was found (A), but strong signals were observed in the area of the IRS at P3, P5, and P7, and in part of the matrix at P3 (B, C, and D). No signal was observed in sections hybridized with sense probe (E). Bars: 50 μm.

kinase-1 (PDK1) upon phosphorylation of their serine/threonine residues in response to signals that stimulate phosphatidylinositol 3-kinase (PI3K).[19,20] Although the functions of SGKL remain largely uncharacterized, the structure of SGKL shows significant similarity to that of protein kinase B (AKT/PKB), including an N-terminal PX or PH domain,[21,22] which is responsible for the subcellular localization of the protein. AKT/PKB is the best-characterized target of phosphatidylinositol 3-kinase (PI3K) lipid products, which regulate cell growth, proliferation, survival, and differentiation.[23,24] Therefore, like AKT/PKB, SGKL is believed to be involved in these cellular processes.

In the present study, we found a nonsense mutation at codon 461 of the *Sgkl* gene resulting in truncation of the C-terminal 35 amino acid residues. It should be noted that the C-terminal end of the protein contains a serine residue (Ser486) that is highly conserved in the AGC subfamily of protein kinases and is phosphorylated in response to signals from PI3K.[16] Nilsen et al. reported that phosphorylation of Ser486 is essential for the interaction between SGKL and PDK1,[25] as mutating Ser486

to Ala prevents the binding of SGKL to PDK1 *in vitro*. Therefore, it is likely that SGKL of *ypc/ypc* mice lacking Ser486 cannot be activated by interacting with PDK1, leading to complete loss of its cellular function. We further revealed that the *Sgkl* gene is expressed specifically in particular cells of the growing hair follicles. These findings clearly indicated that the nucleotide substitution in the *Sgkl* gene is the causative mutation for the defective hair growth seen in *ypc/ypc* mutant mice. Therefore, we termed the mutant allele $Sgkl^{ypc}$.

Although the present findings suggest that SGKL is essential for proper proliferation and differentiation of the cells in hair follicles, the intracellular pathway of SGKL and its downstream molecules remain unclear. Recently, an essential role of the WNT signaling pathway in proliferation and differentiation of cells in the hair follicles has been investigated intensively.[3,9] WNTs are paracrine signaling molecules that regulate cell fate determination, cell adhesive properties, and proliferation.[26] WNTs initiate intracellular signaling by binding to their receptors, *Frizzled* (FZ),[1,26] which inhibits phosphorylation of β-catenin by glycogen syntheses kinase 3 beta (GSK3β and promotes accumulation and nuclear localization of β-catenin. In the nucleus, the accumulated β-catenin activates expression of the target genes that are required for proliferation and differentiation of hair follicles. Recently, Dai et al. reported that SGKL binds to GSK3β and phosphorylates a serine residue of GSK3β to inhibit its kinase activity.[27] These findings suggested that SGKL could modify WNT signaling by inhibition of GSK3β and the lack of function of SGKL in the $Sgkl^{ypc}/Sgkl^{ypc}$ mouse may cause degradation of β-catenin and decreased expression of the target genes in hair follicle cells. Investigation of the phosphorylation of GSK3β and accumulation of β-catenin in the cells of the mutant mice will be required to confirm this hypothesis.

The expression of the *Sgkl* gene has been observed in various tissue, including the lung, colon, heart, and thymus,[15,16] but no apparent abnormalities were observed in these tissues in $Sgkl^{ypc}/Sgkl^{ypc}$ mice except in the hair follicles. As the structure and function of SGKL resembles those of AKT/PKB and both kinases are regulated by PI3K signaling,[16] the lack of SGKL function might be compensated by AKT/PKB or other members of the AGC subfamily of protein kinases in these tissues but not in hair follicles. It should be noted that many molecules implicated in SGKL signaling are associated with carcinogenesis. For example, AKT/PKB is the cellular counterpart of the *v-Akt* oncogene products,[28] overexpression of the WNT gene in the mammary causes adenocarcinoma,[29] APC that forms a complex with GSK3β is a product of the gene responsible for familial adenomatous polyposis (FAP),[30,31] and expression of constitutively stabilized β-catenin in mouse skin results in hair follicle tumors.[32] Therefore, the signaling pathway involving SGKL might be associated with particular types of carcinogenesis and $Sgkl^{ypc}/Sgkl^{ypc}$ mice would have altered characteristics for carcinogenesis.

In the present study, we found restricted expression of the *Sgkl* gene in the IRS and impaired formation of the IRS in the mutant mice. The IRS surrounds the hair shafts beneath the skin surface and is composed of three morphologically distinct cell layers. The precise function of the IRS in hair morphogenesis remains unclear, but it is generally accepted that the IRS provides a supporting structure of the hair follicles, which guide appropriate formation of the hair shafts, including their uniform orientation in the skin.[33] Whether the impaired IRS is the primary cause of the defective hair morphogenesis in the mutant mice is currently unclear, but the present findings demonstrated that the lack of function of SGKL in the cells of the IRS resulted in short, thin, and disorganized hair shafts as well as a lack of their uniform orientation. These findings provide new evidence to support the functional importance of the IRS in hair morphogenesis. Several genes for transcription factors, including *Gata3*,[34] *Cutl1*,[35] and *hr*[36] have been identified as having particular functions in the IRS. For example, expression of the *Gata3* gene in hair follicles is highly restricted to the epidermis and IRS and mice with knockout mutations in the *Gata3* gene showed that IRS progenitors failed to differentiate and IRS could not be formed in the hair follicles.[34] Therefore, GATA-3 is believed to be a key factor for cell fate determination of IRS progenitor cells. Further investigations of the function of SGKL as well as the relationship between SGKL and these transcription factors in the formation of IRS will provide new insight into the function of the IRS in hair follicle morphogenesis.

References

1. Fuchs, E., Merrill, B. J., Jamora, C., and DasGupta, R. 2001, At the roots of a never-ending cycle, *Dev. Cell*, **1**, 13–25.
2. Kishimoto, J., Burgeson, R. E., and Morgan, B. A. 2000, Wnt signaling maintains the hair-inducing activity of the dermal papilla, *Genes Dev.*, **14**, 1181–1185.
3. Millar, S. E., Willert, K., Salinas, P. C. et al. 1999, Wnt signaling in the control of hair growth and structure, *Dev. Biol.*, **207**, 133–149.
4. Mann, G. B., Fowler, K. J., Gabriel, A., Nice, E. C., Williams R. L., and Dunn, A. R. 1993, Mice with a null mutation of the TGFα gene have abnormal skin architecture, wavy hair, and curly whiskers and often develop corneal inflammation, *Cell*, **73**, 249–261.
5. Luetteke, N. C., Qiu, T. H., Peiffer, R. L., Oliver, P., Smithies, O., and Lee, D. C. 1993, TGFα deficiency results in hair follicle and eye abnormalities in targeted and waved-1 mice, *Cell*, **73**, 263–278.
6. Kobielak, K., Pasolli, H. A., Alonso, L., Polak, L., and Fuchs, E. 2003, Defining BMP functions in the hair follicle by conditional ablation of BMP receptor IA, *J. Cell*

Biol., **163**, 609–623.
7. Yuhki, M., Yamada, M., Kawano, M. et al. 2004, BMPR1A signaling is necessary for hair follicle cycling and hair shaft differentiation in mice, *Development*, **131**, 1825–1833.
8. Hébert, J. M., Rosenquist, T., Gotz, J., and Martin, G. R. 1994, FGF5 as a regulator of the hair growth cycle: evidence from targeted and spontaneous mutations, *Cell*, **78**, 1017–1025.
9. Huelsken, J., Vogel, R., Erdmann, B., Cotsarelis, G., and Birchmeier, W. 2001, β-Catenin controls hair follicle morphogenesis and stem cell differentiation in the skin, *Cell*, **105**, 533–545.
10. DasGupta, R. and Fuchs, E. 1999, Multiple roles for activated LEF/TCF transcription complexes during hair follicle development and differentiation, *Development*, **126**, 4557–4568.
11. Stoye, J. P., Fenner, S., Greenoak, G. E., Moran, C., and Coffin, J. M. 1988, Role of endogenous retroviruses as mutagens: the hairless mutation of mice, *Cell*, **54**, 383–391.
12. Luetteke, N. C., Phillips, H. K., Qiu, T. H. et al. 1994, The mouse waved-2 phenotype results from a point mutation in the EGF receptor tyrosine kinase, *Genes Dev.*, **8**, 399–413.
13. Kurosawa, S., Ogura, A., Koura, M. et al. 1991, A histological study on the skin and hairs of PC (poor coat) mice, *Exp. Anim.*, **40**, 259–261.
14. Hung, B. S., Wang, X. Q., Cam, G. R., and Rothnagel, J. A. 2001, Characterization of mouse Frizzled-3 expression in hair follicle development and identification of the human homolog in keratinocytes. *J. Invest. Dermatol.*, **116**, 940–946.
15. Dai, F., Yu, L., He, H. et al. 1999, Cloning and mapping of a novel human serum/glucocorticoid regulated kinase-like gene, SGKL, to chromosome 8q12.3-q13.1, *Genomics*, **62**, 95–97.
16. Kobayashi, T., Deak, M., Morrice, N., and Cohen, P. 1999, Characterization of the structure and regulation of two novel isoforms of serum- and glucocorticoid-induced protein kinase, *Biochem. J.*, **344**, 189–197.
17. Liu, D., Yang, X., and Songyang, Z. 2000, Identification of CISK, a new member of the SGK kinase family that promotes IL-3-dependent survival. *Curr. Biol.*, **10**, 1233–1236.
18. Webster, M. K., Goya, L., Ge, Y., Maiyar, A. C., and Firestone, G. L. 1993, Characterization of sgk, a novel member of the serine/threonine protein kinase gene family which is transcriptionally induced by glucocorticoids and serum, *Mol. Cell. Biol.*, **13**, 2031–2040.
19. Kobayashi, T. and Cohen, P. 1999, Activation of serum- and glucocorticoid-regulated protein kinase by agonists that activate phosphatidylinositide 3-kinase is mediated by 3-phosphoinositide-dependent protein kinase-1 (PDK1) and PDK2, *Biochem. J.*, **339**, 319–328.
20. Park, J., Hill, M. M., Hess, D., Brazil, D. P., Hofsteenge, J., and Hemmings, B. A. 2001, Identification of tyrosine phosphorylation sites on 3-phosphoinositide-dependent protein kinase-1 and their role in regulating kinase activity, *J. Biol. Chem.*, **276**, 37459–37471.
21. Xu, J., Liu, D., Gill, G., and Songyang, Z. 2001, Regulation of cytokine-independent survival kinase (CISK) by the Phox homology domain and phosphoinositides, *J. Cell Biol.*, **154**, 699–705.
22. Virbasius, J. V., Song, X., Pomerleau, D. P., Zhan, Y., Zhou, G. W., and Czech, M. P. 2001, Activationn of the Akt-related cytokine-independent survival kinase requires interaction of its phox domain with endosomal phosphatidylinositol 3-phosphate, *Proc. Natl. Acad. Sci. USA.*, **98**, 12908–12913.
23. Chan, T. O., Rittenhouse, S. E., and Tsichlis, P. N. 1999, AKT/PKB and other D3 phosphoinositide-regulated kinases: kinase activation by phosphoinositide-dependent phosphorylation, *Annu. Rev. Biochem.*, **68**, 965–1014.
24. Downward, J. 1998, Mechanisms and consequences of activation of protein kinase B/Akt, *Curr. Opin. Cell Biol.*, **10**, 262–267.
25. Nilsen, T., Slagsvold, T., Skjerpen, C. S., Brech , A., Stenmark, H., and Olsnes, S. 2004, Peroxisomal targeting as a tool for assaying protein-protein interactions in the living cell: cytokine-independent survival kinase (CISK) binds PDK-1 in vivo in a phosphorylation-dependent manner, *J. Biol. Chem.*, **279**, 4794–4801.
26. Dale, T. C. 1998, Signal transduction by the Wnt family of ligands, *Biochem. J.*, **329**, 209–223.
27. Dai, F., Yu. L., He, H. et al. 2002, Human serum and glucocorticoid-inducible kinase-like kinase (SGKL) phosphorylates glycogen syntheses kinase 3 beta (GSK-3β) at serine-9 through direct interaction, *Biochem. Biophys. Res. Commun.*, **293**, 1191–1196.
28. Staal, S. P. 1987, Molecular cloning of the akt oncogene and its human homologues AKT1 and AKT2: amplification of AKT1 in a primary human gastric adenocarcinoma, *Proc. Natl. Acad. Sci. U.S.A.*, **84**, 5034–5037.
29. Tsukamoto, A. S., Grosschedl, R., Guzman, R. C., Parslow, T., and Varmus, H. E. 1988, Expression of the int-1 gene in transgenic mice is associated with mammary gland hyperplasia and adenocarcinomas in male and female mice, *Cell*, **55**, 619–625.
30. Kinzler, K. W., Nilbert, M. C., Su, L. K. et al. 1991, Identification of FAP locus genes from chromosome 5q21, *Science*, **253**, 661–665.
31. Groden, J., Thliveris, A., Samowitz, W. et al. 1991, Identification and characterization of the familial adenomatous polyposis coli gene, *Cell*, **66**, 589–600.
32. Gat, U., DasGupta, R., Degenstein, L., and Fuchs, E. 1998, De Novo hair follicle morphogenesis and hair tumors in mice expressing a truncated β-catenin in skin, *Cell*, **95**, 605–614.
33. Stenn, K. S. and Paus, R. 2001, Controls of the hair follicle cycling, *Physiol. Rev.*, **81**, 449–494.
34. Kaufman, C. K., Zhou, P., and Pasolli, H. A. 2003, GATA-3: an unexpected regulator of cell lineage determination in skin, *Genes Dev.*, **17**, 2108–2122.
35. Ellis, T., Gambardella, L., Horcher, M. et al. 2001, The transcriptional repressor CDP (Cutl1) is essential for epithelial cell differentiation of the lung and the hair follicle, *Genes Dev.*, **15**, 2307–2319.
36. Panteleyev, A. A., Paus, R., and Christiano, A. M. 2000, Patterns of Hairless (hr) Gene Expression in Mouse Hair Follicle Morphogenesis and Cycling, *Am. J. Pathol.*, **157**, 1071–1079.

THE JOURNAL OF BIOLOGICAL CHEMISTRY
Vol. 279, No. 39, Issue of September 24, pp. 41114–41123, 2004
Printed in U.S.A.

Skeletal Muscle FOXO1 (FKHR) Transgenic Mice Have Less Skeletal Muscle Mass, Down-regulated Type I (Slow Twitch/Red Muscle) Fiber Genes, and Impaired Glycemic Control*[S]

Received for publication, January 21, 2004, and in revised form, July 9, 2004
Published, JBC Papers in Press, July 21, 2004, DOI 10.1074/jbc.M400674200

Yasutomi Kamei‡§¶, Shinji Miura§, Miki Suzuki§, Yuko Kai§, Junko Mizukami‖, Tomoyasu Taniguchi‖, Keiji Mochida, Tomoko Hata‡‡, Junichiro Matsuda‡‡, Hiroyuki Aburatani§§, Ichizo Nishino¶¶, and Osamu Ezaki§**

*From the ‡PRESTO, Japan Science and Technology Agency, §Division of Clinical Nutrition, National Institute of Health and Nutrition, 1-23-1 Toyama, Shinjuku-ku, Tokyo 162-8636, ‖Lead Generation Research Laboratory, Tanabe Seiyaku Co., Ltd., 3-16-89 Kashima, Yodogawa-ku, Osaka 532-8505, **Bioresource Center, Institute of Physical and Chemical Research, 3-1-1 Koyadai, Tsukuba-shi, Ibaraki 305-0074, the ‡‡Department of Veterinary Science, National Institute of Infectious Diseases, 1-23-1 Toyama, Shinjuku-ku, Tokyo 162-8640, §§Research Center for Advanced Science and Technology, University of Tokyo, 4-6-1 Komaba, Meguro-ku, Tokyo 153-8904, and the ¶¶Department of Neuromuscular Research, National Institute of Neuroscience, National Center of Neurology and Psychiatry, 4-1-1 Ogawahigashi-cho, Kodaira, Tokyo 187-8502, Japan*

FOXO1, a member of the FOXO forkhead type transcription factors, is markedly up-regulated in skeletal muscle in energy-deprived states such as fasting and severe diabetes, but its functions in skeletal muscle have remained poorly understood. In this study, we created transgenic mice specifically overexpressing FOXO1 in skeletal muscle. These mice weighed less than the wild-type control mice, had a reduced skeletal muscle mass, and the muscle was paler in color. Microarray analysis revealed that the expression of many genes related to the structural proteins of type I muscles (slow twitch, red muscle) was decreased. Histological analyses showed a marked decrease in size of both type I and type II fibers and a significant decrease in the number of type I fibers in the skeletal muscle of FOXO1 mice. Enhanced gene expression of a lysosomal proteinase, cathepsin L, which is known to be up-regulated during skeletal muscle atrophy, suggested increased protein degradation in the skeletal muscle of FOXO1 mice. Running wheel activity (spontaneous locomotive activity) was significantly reduced in FOXO1 mice compared with control mice. Moreover, the FOXO1 mice showed impaired glycemic control after oral glucose and intraperitoneal insulin administration. These results suggest that FOXO1 negatively regulates skeletal muscle mass and type I fiber gene expression and leads to impaired skeletal muscle function. Activation of FOXO1 may be involved in the pathogenesis of sarcopenia, the age-related decline in muscle mass in humans, which leads to obesity and diabetes.

Skeletal muscle is the largest organ in the human body, comprising about 40% of the body weight. The mass and composition of skeletal muscle are critical for its functions, such as exercise, energy expenditure, and glucose metabolism (1, 2). Elderly humans are known to undergo a progressive loss of muscle fibers associated with diabetes, obesity, and decreased physical activity (sarcopenia) (3). In human skeletal muscle, there are two major classifications of fiber type: type I (slow-twitch oxidative, so-called red muscle) and type II (fast-twitch glycolytic, so-called white muscle) fibers (2). Mass, fiber size, and fiber composition in adult skeletal muscle are regulated in response to changes in physical activity, environment, or pathological conditions. For example, space flight experiments using rats showed a reduction in total skeletal muscle mass of up to 37% as well as a significant loss of contractile proteins in type I but not type II fibers by 1–2 weeks of microgravity (4). Furthermore, the ratio of type I to type II fibers is associated with obesity and diabetes; the number of type I fibers is reduced in obese subjects and diabetic subjects compared with that in controls (5–7).

Skeletal muscle mass is positively regulated by hormones such as insulin-like growth factors (IGFs)[1] and growth hormone (8). Induction of hypertrophy in adult skeletal muscle by increased load is accompanied by the increased expression of IGF-1 (9). Systemic administration of IGF-1 results in increased skeletal muscle protein and reduced protein degradation (10). In addition, overexpression of IGF-1 blocks the age-related loss of skeletal muscle (11). Supplementation of IGF-1 to muscle cells *in vitro* promotes myotube hypertrophy, suggesting that hypertrophy can be mediated by autocrine- or paracrine-produced IGF-1 (12). Thus, delivery of the *IGF-1* gene specifically into skeletal muscle has been proposed as a genetic therapy for skeletal muscle disorders. A better understanding of the role of IGF-1 in skeletal muscle is therefore of great importance.

Specialized/differentiated myofiber phenotypes, including type I and type II fibers, are plastic and are physiologically

* This work was supported in part by research grants from the Japanese Ministry of Health, Labor, and Welfare (Tokyo) and by a grant from the Promotion of Fundamental Studies in Health Sciences of the Organization for Pharmaceutical Safety and Research. The costs of publication of this article were defrayed in part by the payment of page charges. This article must therefore be hereby marked "*advertisement*" in accordance with 18 U.S.C. Section 1734 solely to indicate this fact.

[S] The on-line version of this article (available at http://www.jbc.org) contains Information 1 and 2.

¶ To whom correspondence should be addressed: Division of Clinical Nutrition, National Institute of Health and Nutrition, 1-23-1 Toyama, Shinjuku-ku, Tokyo 162-8636, Japan. Tel.: 81-3-3203-5725; Fax: 81-3-3207-3520; E-mail: ykamei@nih.go.jp.

[1] The abbreviations used are: IGF, insulin-like growth factor; CaMK, calmodulin-dependent kinase; PGC-1α, peroxisome proliferator activated receptor-γ coactivator-1α; STZ, streptozotocin; MLC, myosin light chain; mtCK, mitochondrial creatine kinase; IGFBP, IGF-binding protein; COX, cytochrome *c* oxidase; DEXA, dual energy X-ray absorptiometry; EDL, extensor digitorum longus.

controlled by variations in motor neuron activity. The influence of motor neuron activity on different types of skeletal muscle fibers is considered to be transduced via calcium signaling and downstream molecules such as calcineurin and the calmodulin-dependent kinase (CaMK) pathway (13). Signals generated by calcium/calcineurin/CaMK augment the transactivating function of Mef2 and/or NFAT and enhance type I fiber-specific gene expression (13–18). More recently, it has been shown that a nuclear receptor cofactor (19, 20), peroxisome proliferator activated receptor-γ coactivator-1α (PGC-1α) (21), drives the formation of type I fibers. Specifically, in transgenic mice expressing PGC-1α, type II fibers are red in color, and PGC-1α activates expression of type I fiber-specific genes (22). We also reproduced the PGC-1α-induced red appearance of skeletal muscle; both type I and type II fibers appear redder in transgenic mice overexpressing PGC-1α in skeletal muscle (23).

FOXO1 (FKHR), FOXO4 (AFX), and FOXO3a (FKHRL1) are a subfamily of the forkhead type transcription factors (24, 25). FOXO1 was originally cloned from a rhabdomyosarcoma because of its aberrant fusion with another transcription factor, PAX3, resulting from a chromosomal translocation (26). Recent studies have shown that the FOXO protein can also act as a cofactor of nuclear receptor activity (27–30). FOXO family members have been shown to regulate various cellular functions. FOXOs influence the transcription of genes involved in metabolism (31–34), the cell cycle (35, 36), and apoptosis (37, 38). In addition, FOXO1 can modulate cell differentiation; the constitutive active form of FOXO1 prevents the differentiation of preadipocytes (39) and stimulates myotube fusion of primary mouse myoblasts (40). Moreover, a FOXO1 knockout mouse has been reported; *Foxo1* haploinsufficiency restores insulin sensitivity and rescues the diabetic phenotype in insulin-resistant mice by reducing the hepatic expression of glucogenetic genes and by increasing the adipocytic expression of insulin-sensitizing genes (41). We have shown that FOXO1 expression is increased in skeletal muscle in energy-deprived states, such as in fasting mice, in mice with streptozotocin (STZ)-induced diabetes, and in mice after treadmill running (42). However, the physiological role of FOXO1 in skeletal muscle is still unclear. Although many studies have been performed using cultured cells, studies using animals with genetic modifications focused to the skeletal muscle remain to be conducted in order to understand the function of the FOXO family proteins *in vivo*. Meanwhile, it has been reported that FOXO1 and PGC-1α can physically interact and regulate gene expression in the liver (43). Given that PGC-1α is important for the differentiation of type I fibers, FOXO1 might be involved in this process. (Hereafter, we use "differentiation of muscle fiber" to mean "a switch from one fiber type to another fiber type.") On the other hand, a genetic study of *Caenorhabditis elegans* showed that DAF16, the worm counterpart of FOXO, functions as a suppressor of insulin receptor-like signaling (44). Thus, the FOXO family may act negatively in mammals as a downstream player in insulin or IGF signaling. As IGF-1 plays an important role in controlling skeletal muscle mass, FOXO1 might also be involved in this process.

To gain insight into the potential role of FOXO1 in skeletal muscle, including the control of skeletal muscle mass and the control of differentiation of muscle fiber type, we established transgenic mice specifically overexpressing FOXO1 in their skeletal muscle. Most interestingly, these mice showed reduced skeletal muscle mass, and the muscle was paler in color. Histochemical, physiological, and microarray analyses of these FOXO1 transgenic mice showed that FOXO1 is involved in the regulation of skeletal muscle mass and type I fiber gene expression. In addition, our results suggest that FOXO1 activation may play a role in the impairment of skeletal muscle function including glycemic control.

EXPERIMENTAL PROCEDURES

RNA Analysis—Northern blot analyses were performed as described previously (42). The cDNA probes for Gadd45α (GenBank™ accession number, U00937), troponin C (slow) (M29793), troponin T (slow) (AV213431), myosin light chain (MLC) (slow) (M91602), myoglobin (X04405), mitochondrial creatine kinase (mtCK, AV250974), F_0,F_1-ATPase (AF030559), MLC (fast) (U77943), troponin I (fast) (J04992), troponin T (fast) (L48989), cathepsin L (X06086), IGF-binding protein 5 (IGFBP5) (L12447), MuRF1 (AF294790), and atrogin 1 (AF441120) were obtained by reverse transcription-PCR. The PCR primers used are as follows: Gadd45α, forward, 5′-TCGCACTTGCAATATGACTT-3′, and reverse, 5′-CGGATGCCATCACCGTTCCG-3′; troponin C (slow), forward, 5′-AGCTGCGGTAGAACAGTTGA-3′, and reverse, 5′-TCACCTGTGGCCTGCAGCAT-3′; troponin T (slow), forward, 5′-TTCTGTCCAACATGGGAGCT-3′, and reverse, 5′-TCGGAATTTCTGGGCGTGGC-3′; MLC (slow), forward, 5′-GAGTTCAAGGAAGCCTTCAC-3′, and reverse, 5′-CTGCGAACATCTGGTCGATC-3′; myoglobin, forward, 5′-CACCATGGGGCTCAGTGATG-3′, and reverse, 5′-CTCAGCCCTGGAAGCCTAGC-3′; mtCK, forward, 5′-AAAGGAAGTGGAACGATTAA-3′, and reverse, 5′-TTGATGTCTTGGCCTCTCTC-3′, F_0,F_1-ATPase, forward, 5′-ACTGACCCTGCCCCTGCAAC-3′, and reverse, 5′-CAAGGCTCTTGTGTGGCCTG-3′, MLC (fast), forward, 5′-AGGGATGGCATTATCGACAA-3′, and reverse, 5′-CAGATGTTCTTGTAGTCCAC-3′; troponin I, (fast), forward, 5′-AGGAAAGCCGCCGAGAATCT-3′, and reverse, 5′-TACTGGGGAAGTGGGCAGTT-3′; troponin T (fast), forward, 5′-CAGCAAAGAATTCGCGCTGA-3′, and reverse, 5′-GGCCTTCTTGCTGTGCTTCT-3′; cathepsin L, forward, 5′-CGGAGGAGTCTTACCCCTAT-3′, and reverse, 5′-CTACCCATCAATTCACGACA-3′; IGFBP5, forward, 5′-GCCTATGCCGTACCGGCTCA-3′, and reverse, 5′-CTTCACAGCCTCAGCCTTCA-3′; MuRF1, forward, 5′-ATGAACTTCACGGTGGGTTT-3′, and reverse, 5′-TCAGTGCAGGCCTGAGCCTT-3′; and atrogin 1, forward, 5′-ATGCCGTTCCTTGGGCAGGA-3′, and reverse, 5′-TCAGAACTTGAACAAATTGA-3′. FOXO1, FOXO3a, and FOXO4 cDNA probes were prepared as reported previously (42). COXII, COXIV, Mef2c, PGC-1α, and glucose transporter 4 cDNA probes were prepared as described previously (23). NFAT (IMAGE clone 4109469) and CaMK IIβ (IMAGE clone 5014712) cDNA probes were purchased from Invitrogen.

Generating Transgenic Mice—The human skeletal muscle α-actin promoter (45) was provided by Drs. E. D. Hardeman and K. Guven (Children's Medical Research Institute, Australia). The human FOXO1 cDNA was as described previously (42). The transgene (Fig. 1*A*) was excised from agarose gel and purified for injection (2 ng μl^{-1}). Fertilized eggs were recovered from C57BL/6 females crossed with C57BL/6 males and microinjected at Japan SLC Inc. (Hamamatsu, Japan). The mice were maintained at a constant temperature of 22 °C with fixed artificial light (12-h light and 12-h dark cycle). Care of the mice was conducted in accordance with the institutional guidelines.

Body Composition Analysis—Mice were anesthetized with pentobarbital sodium, Nembutal (0.08 mg/g body weight, Abbott), and scanned with a Lunar PIXI mus2 densitometer (Lunar Corp., Madison, WI), equipped for dual energy x-ray absorptiometry (DEXA) (46).

Immunoblotting—Protein extracts from skeletal muscle were prepared by centrifugation of the tissue homogenates as described previously (47). Protein extracts (30 μg) separated by SDS-PAGE were electrophoretically transferred to Immobilon P membranes (Millipore, Bedford, MA). Immunoblotting was performed by using goat anti-FOXO1 IgG (N-18, Santa Cruz Biotechnology, Inc. Santa Cruz, CA), goat anti-troponin I (slow) (C-19, Santa Cruz Biotechnology), goat anti-troponin I (fast) (C-19, Santa Cruz Biotechnology), goat anti-myoglobin (M-109, Santa Cruz Biotechnology), or rabbit anti-PGC-1α (C terminus, Calbiochem) as primary antibodies (1:1000) and anti-goat IgG or anti-rabbit IgG conjugated with horseradish peroxidase as secondary antibodies (1:1000). Bands were visualized with the enhanced chemiluminescence system (Amersham Biosciences).

Histological Analyses—Skeletal muscle (soleus) samples were frozen in liquid nitrogen-cooled isopentane, and transverse serial sections were stained with ATPase at pH 4.3 to detect type I fibers and at pH 10.5 to detect type II fibers (48). The ratio of type I fibers to type II fibers and the size (area) of skeletal muscle cells were determined by counting cell numbers in six randomly selected cross-section areas (each 900 μm^2) stained with ATPase at pH 4.3.

Blood Analysis—Blood samples were obtained from mice tail tips for hormone and metabolite determination under feeding conditions. Immunoreactive insulin was measured by an insulin assay kit (Morinaga,

Kanagawa, Japan), free fatty acid by NEFA C-test Wako (Wako Biochemicals, Osaka, Japan), lactate by the lactate reagent (Sigma), and glucose by the TIDEX glucose analyzer (Sankyo, Tokyo, Japan).

Running Wheel Activity—Mice were housed individually in cages (9 × 22 × 9 cm) equipped with a running wheel (20-cm in diameter, Shinano Co., Tokyo, Japan). Each wheel revolution was registered by a magnetic switch, which was connected to a counter. The number of revolutions was recorded daily for 6 days.

Oral Glucose and Insulin Tolerance Test—For the oral glucose tolerance test, D-glucose (1 mg/g of body weight, 10% (w/v) glucose solution) was administered with a stomach tube after an overnight fast. Blood samples were obtained by cutting the tail tip before and 30, 60, and 120 min after glucose administration. For the insulin tolerance test, human insulin (Humulin R; Lilly) was injected intraperitoneally (0.75 milliunits/g of body weight) into fed animals. Blood glucose concentrations were measured using a TIDEX glucose analyzer (Sankyo, Tokyo, Japan).

Microarray Analyses—RNA was isolated from skeletal muscle (quadriceps) of sex- and age-matched FOXO1 mice (A1 and A2 lines) and control mice (males at 4 months of age, RNA from three mice of each group were combined). Each of the combined samples was hybridized to the Affymetrix MGU74A microarray, which contains 12,489 genes including ESTs, and analyzed with the Affymetrix Gene Chip 3.1 software as described previously (49). Of the 12,489 genes including ESTs analyzed, 2500 (nontransgenic control mice), 2490 (line A1, transgenic), and 2510 (line A2, transgenic) genes were expressed at a substantial level (absolute call is present and average difference is above 150). Genes were classified on the basis of the biological function of the encoded protein, using a previously established classification scheme (50). The classification scheme was composed of seven major functional categories and several minor functional categories within the major categories.

Statistical Analyses—Statistical comparisons of data from the experimental groups were performed by the one-way analysis of variance, and groups were compared using the Fisher's protected least significant difference test (Statview 5.0, Abacus Concepts, Inc., Berkeley, CA). The glucose and insulin tolerance curves were compared by repeated measure analysis (Statview 5.0, Abacus Concepts). When significant, groups were compared by the Fisher's protected least significant difference test. Statistical significance was defined as $p < 0.05$.

RESULTS

Creation of FOXO1 Mice—The human skeletal muscle α-actin promoter (45) was used to drive the expression of the human *FOXO1* transgene in mice (Fig. 1*A*). During development, cardiac muscle α-actin is the predominant isoform of sarcomeric α-actin in mice, and the switch to skeletal muscle α-actin occurs postpartum (45). Thus, by using the skeletal muscle α-actin promoter, the possibility that embryonic expression of FOXO1 might interfere with development was minimized. We obtained two independent lines of transgenic mice (lines A1 and A2). Southern blot analysis of DNA obtained from mouse tails was performed as shown in Fig. 1*B*. The transgene copy number of each animal was estimated by densitometric scanning of the autoradiographs from the Southern blots.

Expression of the *FOXO1* transgene was evaluated by Northern blot analysis with RNA isolated from the tissues of FOXO1 mice and age-matched control mice at 8 weeks of age (Fig. 1*C*). The use of this promoter resulted in predominantly high expression levels of the *FOXO1* transgene in skeletal muscle (about 3.5 kb). The A2 line showed expression levels of the *FOXO1* transgene in skeletal muscle that were similar to or slightly higher than that in the A1 line. Transgene expression was observed not only in the gastrocnemius and quadriceps but also in other areas of skeletal muscle including the tibialis anterior, extensor digitorum longus (EDL), and soleus (not shown). The blot was then re-hybridized with a cDNA probe of Gadd45α, an authentic target gene of FOXO1 (51, 52). As expected, induction of the expression of Gadd45α was observed in skeletal muscle but not in other tissues in both FOXO1 transgenic mouse lines (Fig. 1*C*), indicating that the transgene expressed a functional FOXO1 protein. By using an antibody that recognizes both human and mouse FOXO1, we confirmed

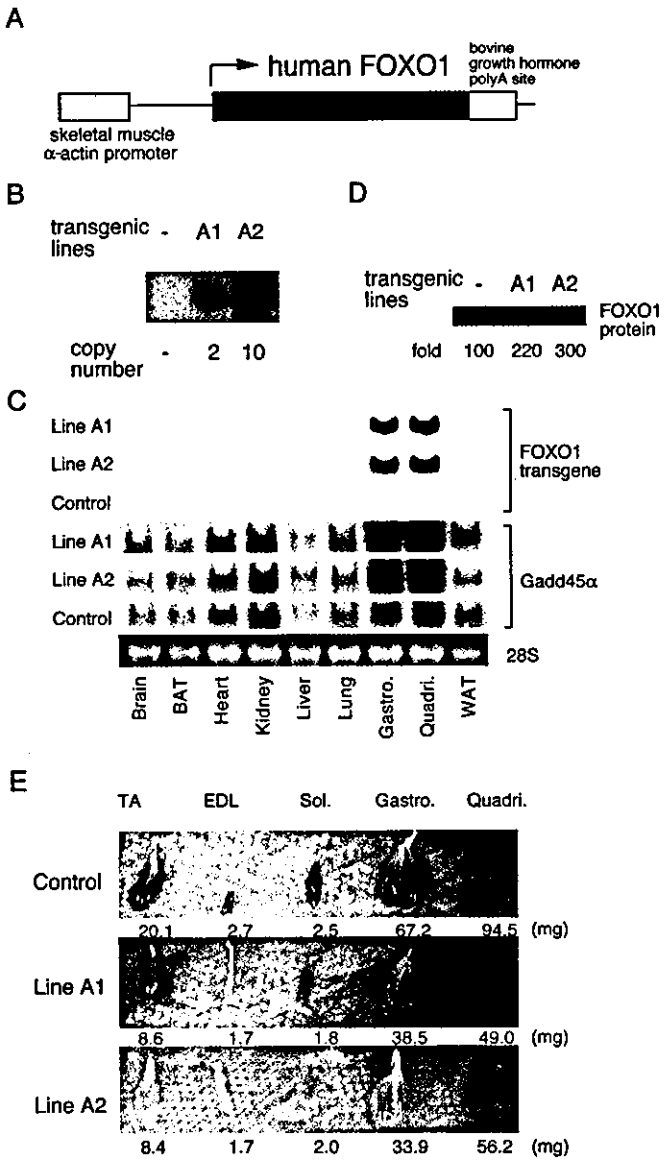

FIG. 1. **Creation of FOXO1 transgenic mice.** *A*, map of the 5-kb construct used for transgenic microinjection. The transgene was under the control of the human skeletal muscle α-actin promoter and included exon 1 and the intron of the human skeletal muscle α-actin gene as well as the bovine growth hormone polyadenylation site (45). *B*, characterization of FOXO1 mice. Two transgenic lines, *A1* and *A2*, were identified by Southern blot analyses of DNA obtained from the tail of each mouse. The copy number was 2 for *A1* and 10 for *A2*, as estimated by densitometric scanning of the autoradiographs of the Southern blot. *C*, expression of the *FOXO1* transgene in mice. Northern blot analysis of human FOXO1 mRNA expression in tissues from FOXO1 mice (*line A1* and *A2*) and nontransgenic control mice. RNAs from brain, brown adipose tissue (*BAT*), heart, kidney, liver, lung, skeletal muscle (gastrocnemius (*Gastro.*) and quadriceps (*Quadri.*)), and white adipose tissue (*WAT*) were analyzed. The blots were re-hybridized with the *Gadd45α* probe. Each lane contained 20 μg of total RNA. *28 S* ribosomal RNA staining of a sample from control mice is shown. Similar staining was observed in samples from transgenic mice (not shown). *D*, expression of the FOXO1 protein in the skeletal muscle of FOXO1 mice. Protein extracts (30 μg per lane) were subjected to SDS-PAGE. The FOXO1 protein was detected by immunoblotting. The densitometric ratio is shown below the autoradiogram (the control was set as *100*). *E*, comparison of representative samples of dissected skeletal muscle (*TA*, tibialis anterior; *Sol*, soleus; *Gastro*, gastrocnemius; *Quadri*, quadriceps) between FOXO1 mice and littermate control mice. Legs were removed from 4-month-old (*lines A1* and *A2*) transgenic mice and age-matched control mice. Tibialis anterior, gastrocnemius, and quadriceps contain a mixture of type I and II fibers; EDL is enriched in type II fibers, and soleus is enriched in type I fibers (control). Average dry mass ($n = 3$ in each group) is shown below the panel. Muscles were smaller in size and paler in color in FOXO1 mice than in control mice.

TABLE I

FOXO1 mice are smaller in body weight and lean body mass

FOXO1 mice weighed less (body weight and lean body mass) than nontransgenic, age- and sex-matched controls, when measured at 5 months of age (line A1) and at 4 months of age (line A2). Fat content per body weight of control and FOXO1 mice did not differ significantly. Data on both male and female mice are shown. Food intake and blood analyses of these mice are also shown. Values represent means ± S.E.

Mice	Numbers	Sex	Age	Body weight	Lean body mass	Fat content	Food intake	Free fatty acid	Lactate	Glucose	Insulin
				g	*g*	%	*g/g/day*	*mEq/liter*	*mg/ml*	*mg/dl*	*pg/ml*
Control	4	Male	5 months	29.0 ± 1.0	24.1 ± 0.3	20.8 ± 1.6	0.18 ± 0.005	0.30 ± 0.025	53.0 ± 4.3	163 ± 2.9	1775 ± 700
A1	4	Male		24.5 ± 0.4[a]	20.3 ± 0.4[b]	20.8 ± 0.5	0.17 ± 0.004	0.34 ± 0.098	56.3 ± 8.3	173 ± 14	739 ± 139
Control	4	Female		21.6 ± 0.9	19.3 ± 0.9	12.9 ± 1.0	0.25 ± 0.017	0.39 ± 0.060	32.7 ± 3.1	158 ± 8.0	289 ± 14
A1	6	Female		18.4 ± 0.4[a]	16.4 ± 0.2[a]	15.8 ± 1.2	0.24 ± 0.017	0.38 ± 0.049	38.9 ± 2.5	163 ± 5.3	302 ± 5
Control	4	Male	4 months	24.3 ± 0.4	21.0 ± 0.4	15.2 ± 1.2	0.21 ± 0.011	0.40 ± 0.045	37.3 ± 3.7	160 ± 10	373 ± 19
A2	4	Male		19.4 ± 0.1[b]	17.4 ± 0.2[b]	15.0 ± 1.9	0.18 ± 0.017	0.33 ± 0.077	46.4 ± 6.6	184 ± 14	573 ± 109
Control	4	Female		19.9 ± 0.6	17.6 ± 0.7	12.8 ± 0.2	0.25 ± 0.027	0.45 ± 0.055	34.5 ± 1.9	144 ± 10	283 ± 10
A2	4	Female		17.3 ± 0.3[a]	15.1 ± 0.4[c]	13.3 ± 0.9	0.23 ± 0.041	0.58 ± 0.096	35.7 ± 5.9	143 ± 6.5	316 ± 10

[a] $p < 0.01$.
[b] $p < 0.001$.
[c] $p < 0.05$.

the presence of the FOXO1 protein in the skeletal muscle of FOXO1 mice (Fig. 1*D*). An ~2.2-fold (line A1) and 3-fold (line A2) increase in FOXO1 protein levels was observed. These increases were at the physiological level, since 24-h fasting has been shown to increase FOXO1 protein content by 2.5–3-fold (Ref. 53 and data not shown).

FOXO1 Mice Are Small—The apparent phenotype observed in FOXO1 mice was small stature and thinner legs than the control mice. Both male and female transgenic mice weighed about 10% less than the control mice at 5 weeks of age (not shown). We used DEXA to measure the lean body mass (body weight excluding fat weight) and the content of fat in the whole body of the A1 line (at 5 months of age) and the A2 line (at 4 months of age) in age- and sex-matched control mice (Table I). Both body weight and lean body mass were significantly lower in both male and female FOXO1 mice (both lines) than in control mice. However, the fat content per total body weight of both FOXO1 mouse lines was comparable with that of nontransgenic mice (Table I). Thus, the decrease in body weight of the FOXO1 mice is not caused by a decrease in body fat but by a decrease in lean body mass. Consistent with the data on decreased lean body mass, the skeletal muscles in FOXO1 mice were smaller in size and dry mass, as well as paler in color than those of control mice (Fig. 1*E*). Consumption of food per body weight was not significantly different between FOXO1 mice and control mice (Table I). Blood metabolite (free fatty acid, lactate, and glucose) and insulin levels did not differ significantly between FOXO1 mice and the controls (Table I).

Microarray Analysis—To obtain information on changes in gene expression in FOXO1 mice, we performed microarray analysis using RNA samples from skeletal muscle (quadriceps) of transgenic and control mice. Most interestingly, the largest category of genes with suppressed expression in the transgenic mice was those involved in cell structure. Namely, about half of the down-regulated genes were classified as cytoskeletal proteins (Table II). The FOXO1-induced genes were distributed throughout various categories (not shown, see Supplemental Material 1).

In the skeletal muscle of FOXO1 mice, there was a decrease in the expression levels of genes related to structural proteins of the type I fiber (slow twitch oxidative, red muscle), such as slow muscle isoforms of myosins (Table II, line numbers 1, 4, and 6), slow isoforms of troponins (Table II, line numbers 2, 5, and 7), α-tropomyosin slow type (Table II, line number 13), myoglobin (Table II, line number 12), and mtCK (Table II, line number 15), which are abundant in type I fibers (54). This is consistent with the observation that the skeletal muscles of FOXO1 mice are pale (Fig. 1*E*). In the microarray, the expression of mitochondrial oxidative metabolism genes, such as the electron transport system, did not differ between FOXO1 mice and controls (not shown). In large mammals such as humans, type I fibers are higher in mitochondrial content and more dependent on oxidative metabolism than type II fibers. In small mammals (*e.g.* mouse and rat), a large amount of mitochondria is seen in type II fibers as well as type I fibers (2). The large amount of mitochondria in both type I and type II fibers in mice would explain the unchanged gene expression of the mitochondrial electron transport system, although expression of type I fiber genes was markedly suppressed. In addition, the gene expression of type II fiber isoforms did not differ (not shown). Namely, expression of genes preferentially abundant in type I fibers appears to be suppressed in the skeletal muscle of FOXO1 mice.

Northern Blot Analysis of Representative Genes—We recognize the limitation of single microarray assays, as they can contain certain noise in the data. Thus, to verify the changes of gene expression found in the microarray analysis, we performed Northern blot analysis by using probes for several genes. In addition to representative genes in the list (Table II), we also analyzed several additionally selected genes of type I fiber or type II fiber markers or genes that may be involved in fiber differentiation. FOXO1 overexpression did not significantly affect mRNA levels of the other FOXO members, FOXO4 and FOXO3a (Fig. 2*A*). Consistent with the microarray data, a reduction in gene expression was confirmed for type I fiber proteins, such as troponin C (slow) (Table II, line number 2), MLC (slow) (Table II, line number 6), troponin T (slow) (Table II, line number 7), myoglobin (Table II, line number 12), and mtCK (Table II, line number 15) (Fig. 2*A*). On the other hand, expression levels of genes for components of the mitochondrial electron transport system, such as cytochrome *c* oxidase II and IV (COX II and IV), and the F_0,F_1-ATPase, were not markedly changed in the skeletal muscle of FOXO1 mice. Next, we examined type II fiber genes. The expression of genes for troponin I (fast), troponin T (fast), and MLC (fast) did not differ between FOXO1 mice and control mice. Thus, the results of the microarray analysis were confirmed by Northern blot analysis. In addition, given that Mef2, NFAT, CaMK, and PGC-1α have been implicated recently in regulating gene expression in type I fibers (14–18, 22), we also examined the level of their expression in skeletal muscle of control and FOXO1 mice. PGC-1α mRNA levels were slightly increased in the skeletal muscle of FOXO1 mice (line A2). Most interestingly, expression levels of Mef2c and CaMK were reduced in FOXO1 mice. FOXO1-mediated down-regulation of type I fiber genes may, in part, be regulated by Mef2c and CaMK.

Moreover, we examined the expression levels of genes whose expression levels are known to be changed during skeletal

TABLE II

Gene with decreased expression in the skeletal muscle of FOXO1 mice

The expression levels of 22 genes were significantly decreased in both the A1 and A2 lines of FOXO1 mice. The genes are listed in the order of greatest fold change in expression in skeletal muscle from line A1 mice relative to control mice. Fold change calculations were carried out as an indication of the relative change of each transcript represented on the probe array. The average difference value is a marker of abundance of each gene. Categories and subcategories are based on a previously established classification scheme (50) and literature review. Change (↓) indicates that expression is significantly decreased compared with control mice.

	GenBank™ accession no.	Gene description	Categories	Subcategories	Fold change (line A1)	Fold change (line A2)	Average difference (control)	Average difference (line A1)	Average difference (line A2)
1	AJ223362	Myosin, heavy polypeptide 7, cardiac muscle, β	Cell structure	Cytoskeletal	−57.6↓	−41.8↓	418	−97	10
2	M29793	Troponin C (cardiac/slow skeletal isoform)	Cell structure	Cytoskeletal	−30.4↓	−9.7↓	260	2	39
3	U88623	Aquaporin 4	Metabolism	Transport	−21↓	−10.2↓	259	10	21
4	X12972	Myosin alkali light chain (ventricular/slow muscle isoform)	Cell structure	Cytoskeletal	−6.8↓	−2.1↓	937	129	450
5	AJ242874	Troponin I, skeletal, slow 1	Cell structure	Cytoskeletal	−6.7↓	−3.2↓	313	48	109
6	M91602	Myosin light chain 2 (cardiac ventricle isoform)	Cell structure	Cytoskeletal	−5.8↓	−3↓	1038	165	316
7	AV213431	Troponin T1 (slow twitch isoform)	Cell structure	Cytoskeletal	−4.4↓	−3.1↓	772	174	246
8	M74570	Aldehyde dehydrogenase II	Metabolism	Sugar/glycolysis	−4↓	−2.8↓	567	140	209
9	U34277	Platelet-activating factor acetylhydrolase	Cell defense	Homeostasis	−3.1↓	−2↓	238	77	120
10	AI646638	Clone MGC:37615 IMAGE: 4989784, mRNA,	Not found in the list		−2.9↓	−2.2↓	150	51	68
11	D45203	Pentylenetetrazole-related mRNA PTZ-17	Not found in the list		−2.8↓	−3↓	1232	434	411
12	X04405	Myoglobin	Cell defense	Homeostasis	−2.8↓	−1.8↓	2484	812	1410
13	U04541	Tropomyosin 3 (slow twitch isoform)	Cell structure	Cytoskeletal	−2.7↓	−2.4↓	662	243	273
14	X92665	Ubiquitin-conjugating enzyme E2E1	Protein expression	Post-translational modification	−2.1↓	−1.7↓	298	187	175
15	AV250974	Creatine kinase, mitochondrial 2	Metabolism	Sugar/ glycolysis	−2↓	−1.8↓	671	300	339
16	X57349	Transferrin receptor	Cell defense	Homeostasis	−1.9↓	−2.8↓	276	121	82
17	L12447	Insulin-like growth factor-binding protein 5	Unclassified		−1.9↓	−1.9↓	2080	1111	1095
18	Z38015	Myotonin protein kinase	Cell signaling	Protein modification	−1.9↓	−1.8↓	684	361	374
19	AB010144	Mitsugumin29, a synaptophysin family	Cell structure	General	−1.8↓	−2.4↓	742	414	312
20	X63615	Calcium/calmodulin-dependent protein kinase II, β	Cell signaling	Protein modification	−1.8↓	−2.1↓	295	160	146
21	U00677	Syntrophin, acidic 1	Cell structure	Cytoskeletal	−1.7↓	−1.7↓	857	504	491
22	AF032099	Potassium voltage-gated channel	Cell signaling	Channel/transport	−1.5↓	−1.6↓	320	209	195

muscle atrophy such as caused by fasting, cachexia, and STZ-induced diabetes (55). Specifically, gene expression of atrogin 1/MAFbx, MuRF1 (both are ubiquitin ligases), and cathepsin L (a lysosomal protease) is up-regulated and IGFBP5 is down-regulated during skeletal muscle atrophy (55). In our Northern blot analysis, the level of atrogin 1 expression was increased in the A2 line of FOXO1 mice, which has less skeletal muscle, but not in the A1 line, which also has less skeletal muscle mass than nontransgenic controls. In both the A1 and A2 lines of FOXO1 mice, the expression of cathepsin L and IGFBP5 was increased and decreased, respectively. The MuRF1 mRNA level was not changed. Thus, atrophy-related gene expression changes including that of protein degradation likely occurred in the skeletal muscle of FOXO1 mice.

Western Blot Analysis of the Skeletal Muscle of FOXO1 Mice and PGC-1α Mice—We examined the expression of various gene products of FOXO1 mice at the protein level by Western blot analysis (Fig. 2*B*). Protein extracts from the skeletal muscle of FOXO1 mice (A1 and A2 lines) and wild-type control mice were used. For comparison, we analyzed protein extracts from the skeletal muscle of PGC-1α transgenic mice, which we previously analyzed (23). Protein levels of troponin I (slow) and myoglobin, which are rich in type I fibers, were increased in PGC-1α mice but decreased in FOXO1 mice (Fig. 2*B*). On the other hand, the protein level of troponin I (fast), which is rich in type II fibers, was decreased in PGC-1α mice but not in FOXO1 mice (Fig. 2*B*). Thus, Western blot analysis of the protein expression of genes for type I and type II fibers was consistent with the results of mRNA expression analysis.

Histological Analysis of Skeletal Muscle of FOXO1 Mice—We examined the relationship between the change in type I fiber gene expression and actual muscle fiber morphology in the skeletal muscle (soleus) of transgenic mice using light microscopy and histochemical procedures (A1 line, 4 months after birth; A2 line, 3 months after birth). Distinction between type I and type II fibers can be made by myosin ATPase staining at different pH values. Specifically, at pH 10.5, type II fibers are well stained but not type I fibers, and at pH 4.3, type I fibers are well stained but not type II fibers (2). ATPase staining revealed that skeletal muscle cells (both type I and type II fibers) in the FOXO1 mice are smaller than those of the control mice (average cross-sectional area of muscle fibers; A1 line, 11.5 ± 0.8 μm^2 in FOXO1 mice and 20.0 ± 2.7 μm^2 in control mice; A2 line, 9.8 ± 0.5 μm^2 in FOXO1 mice and 14.1 ± 1.9 μm^2 in control mice) and had fewer type I fibers than those in the control mice (average; A1 line, 28.6 ± 1.3% in FOXO1 mice and

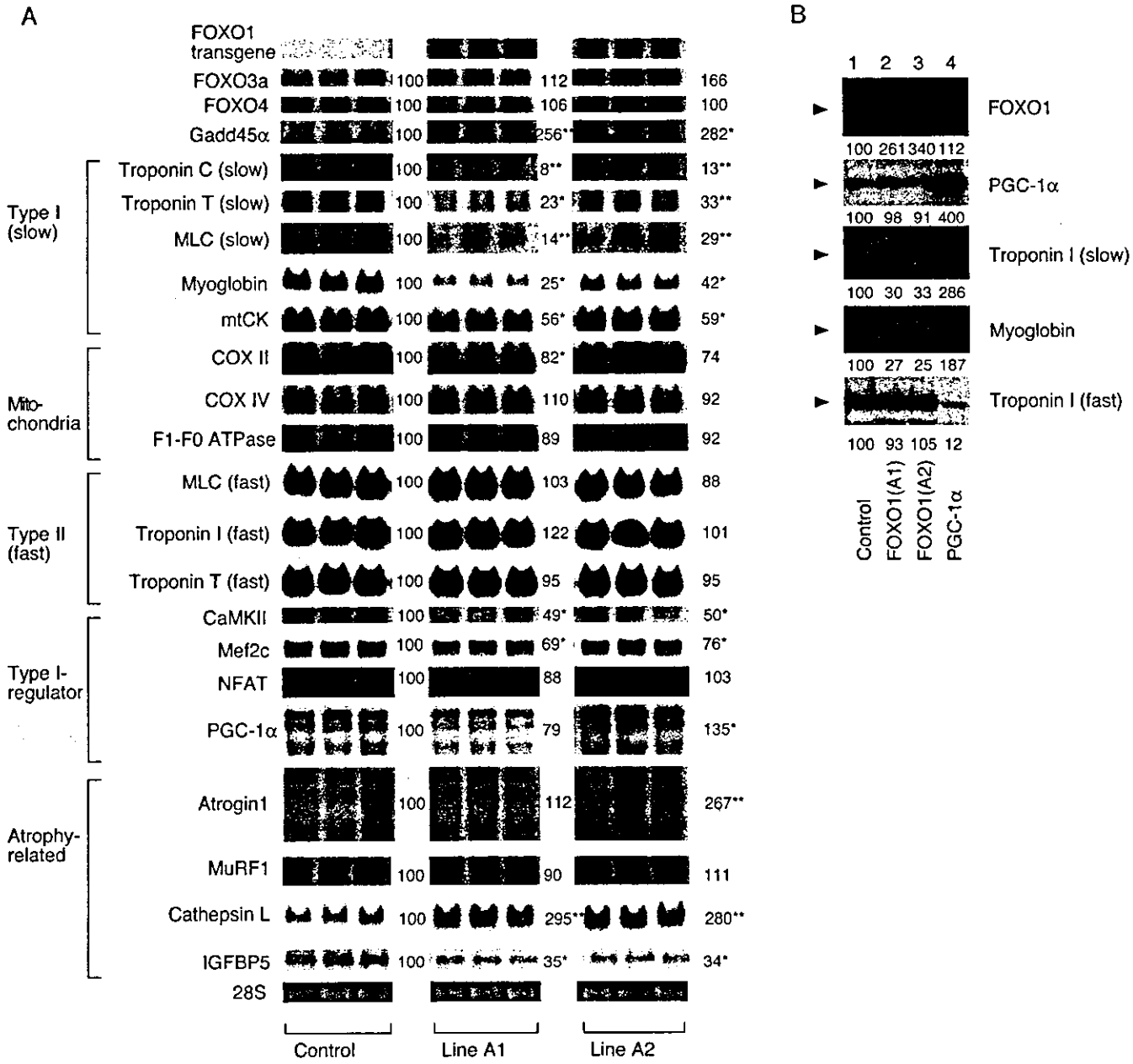

FIG. 2. **Gene product levels in the skeletal muscle of FOXO1 mice.** *A*, Northern blot analysis was performed on total RNA (20 μg per lane) isolated from skeletal muscle (quadriceps) of FOXO1 mice (*line A1* and *line A2*) and nontransgenic control mice. The same RNA sample sets were blotted onto multiple membranes and hybridized with the indicated probes. The names of genes examined are on the *left* of the autoradiograms, and average densitometric ratios (the control was set as *100*) are on the *right* (*, $p < 0.05$; **, $p < 0.01$). Equal sample loading was confirmed by ethidium bromide staining of 28 S ribosomal RNA. Each lane represents a sample from an individual mouse. *B*, Western blot analysis was performed on protein extracts from the skeletal muscle of *FOXO1* mice (*A1* and *A2* lines), PGC-1α mice, and control mice. Antibodies against FOXO1, PGC-1α, troponin I (slow), myoglobin, and troponin I (fast) were used. A typical autoradiogram, representative of three independent experiments with similar results, is shown. *Numbers* below the panels are values of the densitometric ratios (the signal of the control for each sample was set as *100*). Corresponding bands are indicated by *arrowheads*. The approximate estimated molecular sizes are as follows: FOXO1, 70 kDa; PGC-1α, 90 kDa; troponin I (slow), 30 kDa; myoglobin, 30 kDa; and troponin (fast), 40 kDa.

37.8 ± 2.2% in control; A2 line, 20.2 ± 2.3% in FOXO1 mice and 40.4 ± 2.0% in control) (Fig. 3*A*). Immunohistochemistry with antibodies to myoglobin (present at high concentrations in type I fibers) confirmed the reduction in the number of type I fibers in the skeletal muscle of FOXO1 mice (not shown). Skeletal muscle samples from FOXO1 mice had no structural abnormalities such as mitochondrial abnormalities, glycogen accumulation, vacuolar formation, and muscle fiber degeneration (not shown).

Running Wheel Activity of FOXO1 Mice—The mass and fiber composition of skeletal muscle are important for physical exercise. Type I fibers are more resistant to fatigue than type II fibers (2). As the FOXO1 mice had decreased total skeletal muscle mass and fewer type I fibers, they may have a low capacity for endurance, such as that needed in a marathon. We then compared the running wheel activity (spontaneous locomotive activity) in FOXO1 mice and control mice. Mice were transferred to cages with a running wheel and monitored daily for the number of wheel revolutions made for 6 days. Both lines of FOXO1 mice showed significantly fewer wheel revolutions (Fig. 3*B*). The decrease in running wheel activity suggested that FOXO1 mice were less able to sustain continuous muscle

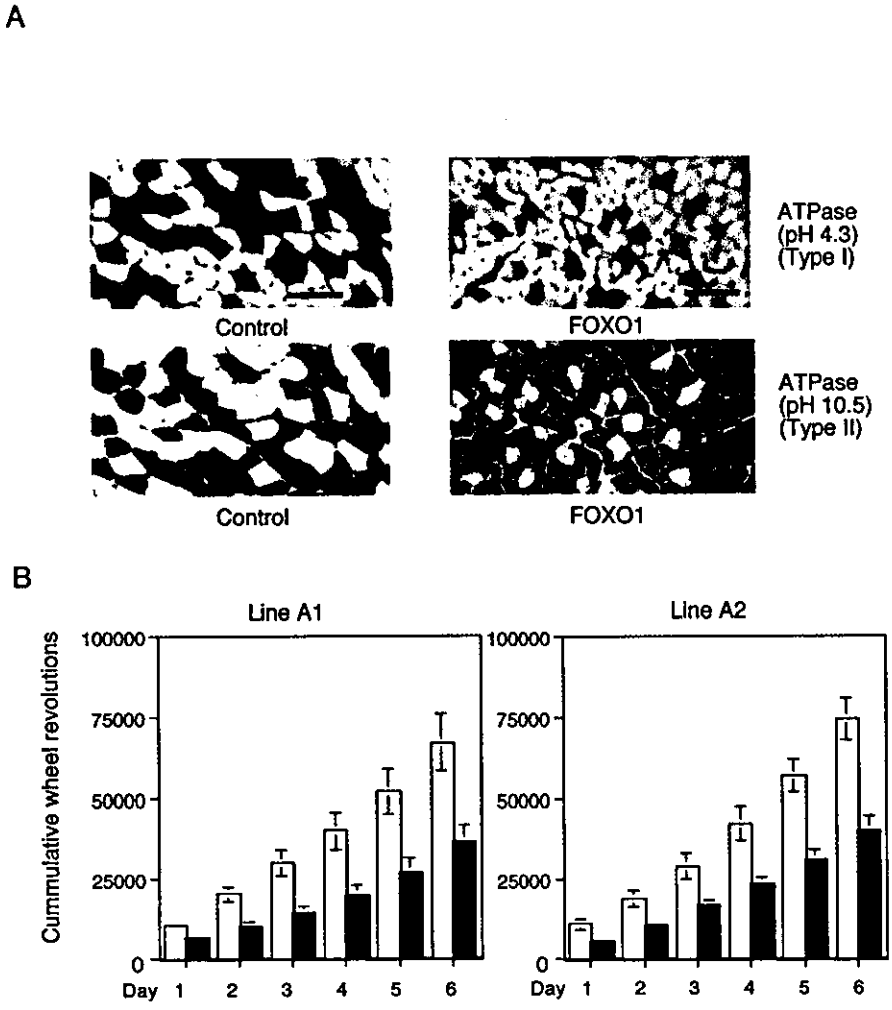

FIG. 3. *A*, histological analysis of skeletal muscle. Light microscopy of ATPase (pH 4.3 for type I fibers and pH 10.5 for type II fibers)-stained transverse sections of skeletal muscle (soleus) specimens from FOXO1 mice (line A2) and control littermates at 3 months of age. *Bars*, 50 μm. Skeletal muscle fibers of *FOXO1* mice were thinner and contained fewer type I fibers than that of control mice. *B*, running wheel activity of FOXO1 mice. Mice were housed individually in cages equipped with a running wheel (20 cm in diameter). The number of revolutions made was recorded daily for 6 days, and the cumulative values are shown. *Open column*, control; *closed column*, FOXO1 mice. Running wheel activity was significantly ($p < 0.05$) reduced in FOXO1 mice (*line A1, left*; *line A2, right*) compared with control mice. Mice used were females at 10 weeks (*line A1*) and 9 weeks (*line A2*) of age. Numbers of animals used are as follows: line A1, control, $n = 6$; FOXO1 mice, $n = 5$; line A2, control, $n = 4$; FOXO1 mice, $n = 3$. Because male mice responded similarly, only the data from female mice are shown. *C* and *D*, oral glucose tolerance tests (*C*) and insulin tolerance tests (*D*) on FOXO1 mice. For the oral glucose tolerance test, mice were fasted overnight and given D-glucose (1 mg/g body weight) orally by a stomach tube. Blood glucose levels were determined at the times indicated. For the insulin tolerance test, mice were allowed free access to food and then given 0.75 milliunits of human insulin/g of body weight. Blood glucose levels were measured at the indicated time points. Mice used were males at 10 weeks (line A1) and 9 weeks (line A2) of age. The numbers of animals used were: *line A1*, control, $n = 6$; FOXO1 mice, $n = 5$; *line A2*, control, $n = 5$; FOXO1 mice, $n = 4$.

contractions than control mice, which is consistent with the reduction in the mass of skeletal muscle and the number of type I fibers.

Oral Glucose Tolerance Test and Insulin Tolerance Test on FOXO1 Mice—Skeletal muscle is important for glucose metabolism. To examine whether the decreased skeletal muscle mass of FOXO1 mice is affecting their systemic glucose homeostasis, we examined oral glucose tolerance and insulin tolerance in FOXO1 mice. Glucose tolerance was impaired in both lines of FOXO1 mice, namely peak blood glucose values in FOXO1 mice were elevated significantly above those of the control mice (Fig. 3*C*). The insulin tolerance test clearly demonstrated that the glucose-lowering effects of insulin were impaired in both the A1 and A2 lines of FOXO1 mice, compared with those in age- and sex-matched control mice (Fig. 3*D*). FOXO1 mice showed a low capacity for glucose metabolism and decreased insulin sensitivity. Adipose tissue, another organ playing a role in glucose metabolism, appears not to be involved in this impaired glycemic control because 1) body fat did not differ between FOXO1 mice and control mice (Table I), and 2) gene expression of glucose transporter 4, which is a rate-limiting molecule of insulin-dependent glucose intake (56), was not decreased in adipose tissue of FOXO1 mice (see Supplemental Material 2). FOXO1 mice may therefore represent a certain type of diabetic state in humans.

Change in Endogenous FOXO1 Expression by Physical Inactivity—We performed Northern blot analysis with RNA from the skeletal muscle of mice maintained under a long period of physical inactivity. The right hindlimbs of wild-type mice were immobilized in plaster casts, and the left hindlimbs were left freely moving for the control sample. After 3 weeks in the plaster casts, skeletal muscle (gastrocnemius) weight of the right hindlimbs was significantly decreased compared with that in the controls (average, 88 ± 12 mg for immobilized and 149 ± 6 mg for freely moving controls, $n = 3$, $p < 0.05$). As shown in Fig. 4, the gene expression of troponin C (slow), myoglobin, and mtCK but not MLC (fast) and troponin T (fast) was markedly decreased in the plaster-casted muscle. At the same time, endogenous FOXO1 mRNA was increased in the immobilized muscle (Fig. 4). Furthermore, Gadd45α was increased in the same sample. In addition, cathepsin L, but not atrogin 1 and MuRF1, were increased (Fig. 4). Thus, mRNAs of endogenous FOXO1, Gadd45α, and cathepsin L were increased; skeletal muscle mass was decreased, and the expression of type I fiber genes but not type II fiber genes were decreased. The gene expression changes observed in the plaster-casted skeletal muscle were similar to the changes observed in the FOXO1 mice (Fig. 2*A*). These results further support the involvement of FOXO1 in the negative regulation of skeletal muscle mass and the expression of type I fiber genes.

DISCUSSION

To gain insight into the role of FOXO1 in skeletal muscle *in vivo*, we established transgenic mice overexpressing human FOXO1. The *FOXO1* transgene was predominantly expressed in the skeletal muscle, and the increase in FOXO1 protein expression was within physiological levels. Most interestingly, the skeletal muscle of FOXO1 mice weighed less and was paler

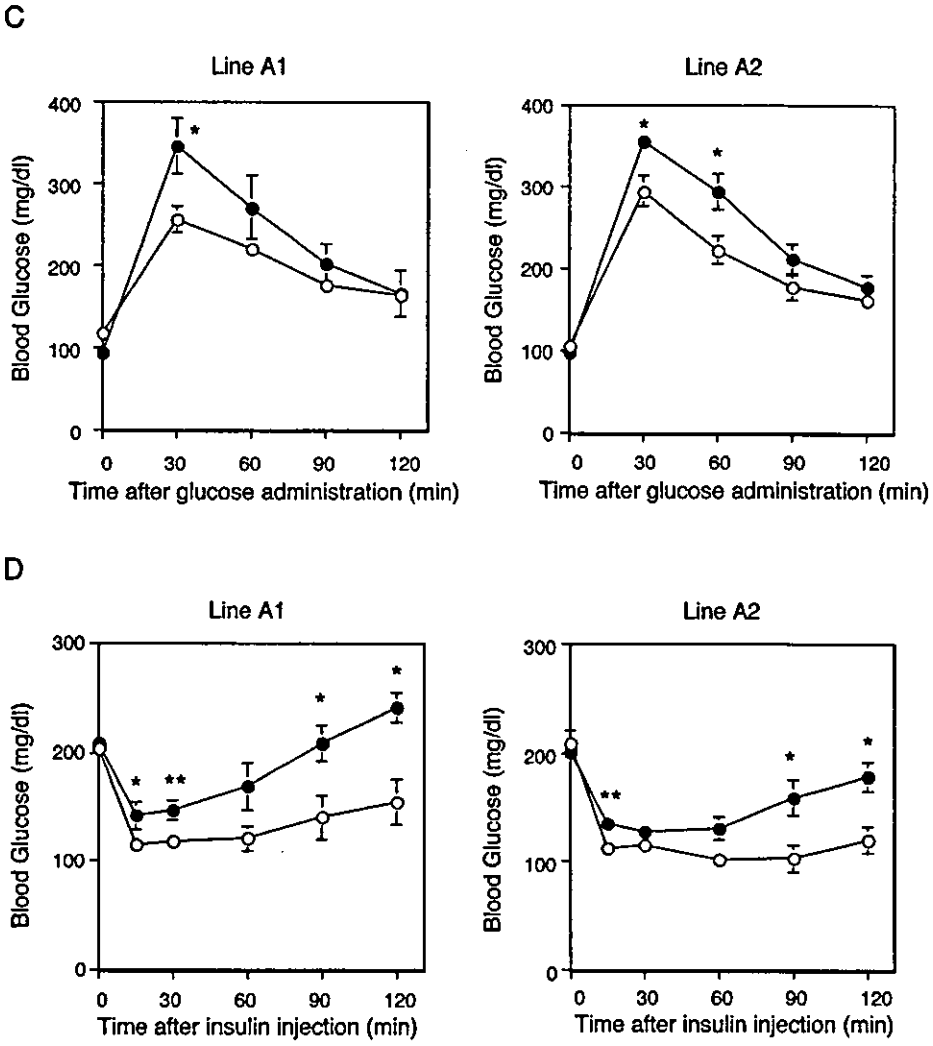

FIG. 3—*continued*

in color. The results of gene expression analyses showed that type I (red muscle) fiber-related gene expression was decreased in the skeletal muscle of FOXO1 mice. In addition, histological examinations showed that the skeletal muscle of FOXO1 mice had fewer type I fibers and smaller type I and type II fibers. Consistently, under long time physical inactivity by immobilizing skeletal muscle in plaster casts, an increased expression of endogenous FOXO1 mRNA and a markedly decreased expression of genes related to type I fibers were observed. These results suggest that FOXO1 is a negative regulator of skeletal muscle mass and expression of type I fiber-related genes. Moreover, FOXO1 mice showed poor glycemic control and low capacity for physical exercise, which involves the skeletal muscles, especially type I fibers. These phenotypes are consistent with the decreased mass of skeletal muscle including type I fibers in FOXO1 mice.

How does FOXO1 affect the skeletal muscle, including the reduction of mass of both type I and type II fibers and the suppressed expression of type I fiber genes? In the following, we discuss the possibility of involvement of FOXO1 in 1) growth, 2) protein degradation, and 3) differentiation of skeletal muscle.

1) FOXO1 may suppress increase of skeletal muscle mass. A genetic study of *C. elegans* showed that DAF16, the worm counterpart of FOXO, functions as a suppressor of insulin receptor-like signaling (44). Thus, the FOXO family might act negatively in mammals as a downstream player in insulin or IGF signaling. IGF-1 stimulates the proliferation of skeletal muscle satellite cells (57). Mature skeletal muscle fibers are not able to proliferate. Skeletal muscle satellite cells, mononuclear cells located between the basement membrane and the plasma membrane of myofibers in mature cells, are important in postnatal skeletal muscle hypertrophy because of their ability to add new myonuclei into growing myofibers. Machida *et al.* (58) showed that FOXO1 inhibited IGF-1-mediated skeletal muscle cell proliferation. In primary skeletal muscle satellite cells, FOXO1 activates the promoter of p27 Kip1, an inhibitor of the cell cycle at the G_1 stage, which leads to inhibition of cell proliferation, and addition of IGF-1 reverses the FOXO1-mediated activation of the p27 Kip1 promoter (58). Unexpectedly, p27 Kip1 mRNA expression was unchanged in the skeletal muscle of FOXO1 mice compared with that of controls (not shown). As the ratio of satellite cells is very small in total skeletal muscle, the increased expression of p27 Kip1 in satellite cells may not have been detected in our assay. On the other hand, we showed enhanced expression of Gadd45α, an inhibitor of the cell cycle at the G_2 stage (51, 52), in the skeletal muscle of FOXO1 mice (Figs. 1 and 2*A*). As a 0.7-kb stretch of the rat skeletal muscle α-actin promoter is active in skeletal muscle satellite cells (59), the *FOXO1* transgene, driven by a 2-kb stretch of the human skeletal muscle α-actin promoter (45), is likely to be expressed in the skeletal muscle satellite cells of the FOXO1 mice. Thus, the increased amount of Gadd45α and possibly p27 Kip1 in the skeletal muscle satellite cells of FOXO1 mice may have suppressed the proliferation of satellite cells and caused a decrease in skeletal muscle mass (size).

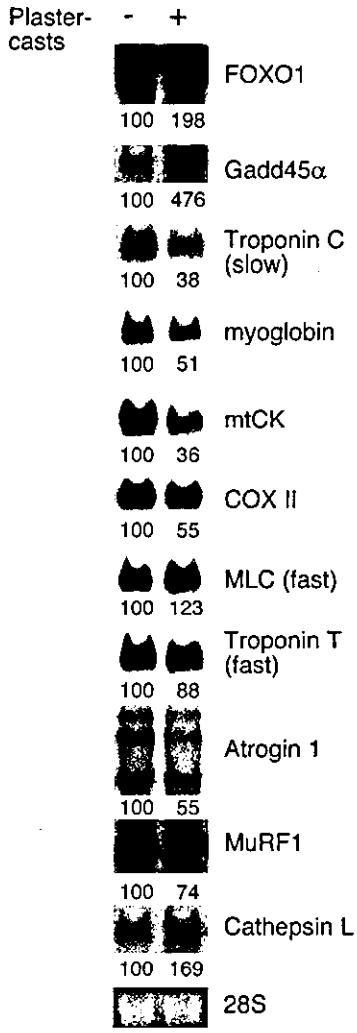

FIG. 4. **Gene expression in skeletal muscle immobilized in plaster casts.** The right hindlimbs of mice at 9 weeks of age were immobilized in plaster casts, and left hindlimbs of the mice were kept free for the control sample. After 3 weeks of immobilization in plaster casts, Northern analysis was performed on total RNA (20 μg per lane) isolated from the skeletal muscle (gastrocnemius) of right hindlimbs and left hindlimbs. *Plus* and *minus* denote with or without immobilization, respectively. The names of the genes examined are on the *right* of the autoradiograms. A typical autoradiogram, representative of three independent mice with similar results, is shown. The densitometric ratio is shown *below* the autoradiograms (the control was set as *100*).

2) FOXO1 may increase the degradation rate of skeletal muscle proteins. Gene expression of atrogin 1, MuRF1 (both are ubiquitin ligases), and cathepsin L (a lysosomal protease) is up-regulated and IGFBP5 is down-regulated during skeletal muscle atrophy caused by fasting, cachexia, STZ-induced diabetes, and other diseases (55). After we submitted our manuscript, a member of the FOXO family, FOXO3a, was reported to activate the gene expression of atrogin 1, and addition of IGF-1 was found to reverse the FOXO3a-mediated activation of the atrogin 1 promoter (60). Overexpression of an active form of FOXO3a reduces the size of skeletal muscle fibers, both *in vivo* and *in vitro* (60). In addition, another group reported that overexpression of an active form of FOXO1 in C2C12 muscle cells did not change the base-line expression of atrogin 1 and MuRF1, but the active form of FOXO1 suppresses IGF-1-mediated repression of atrogin 1 and MuRF1 expression induced by glucocorticoids (61). This suggests that FOXO1 expression is not sufficient for inducing atrophy-related genes, but FOXO1 is negatively involved in IGF-1-mediated suppression of atrophy of skeletal muscle. In our Northern blot analysis, the level of atrogin 1 was increased in the A2 line but not in the A1 line of FOXO1 mice, although both had less skeletal muscle mass than the nontransgenic controls. In both the A1 and A2 lines of FOXO1 mice, the expression of cathepsin L and IGFBP5 was increased and decreased, respectively. MuRF1 mRNA levels were not altered in both lines. Thus, atrophy-related protein degradation probably occurs in the skeletal muscle of FOXO1 mice and could explain, in part, the decrease in skeletal muscle mass of the FOXO1 mice. However, the increase in atrogin 1 is unlikely to be enough to cause the decrease in skeletal muscle mass of FOXO1 mice, because the expression level did not change in the A1 line of FOXO1 mice. This is consistent with the description by Sandri *et al.* (60) that overexpression of atrogin 1 alone does not cause myotube or muscle atrophy. On the other hand, IGFBP5 is reported to modulate the activity of IGF-1 (62), and hence decreased expression of IGFBP5 may contribute to the decrease in skeletal muscle mass by affecting IGF-1 action. *FOXO1* transgene expression was observed in both type I fiber-rich soleus and type II fiber-rich EDL. Thus, changes in the expression of atrophy-related genes may be an alternative molecular explanation for the decreased skeletal muscle mass, including the size of both type I and type II fibers of FOXO1 mice.

3) Does FOXO1 inhibit the differentiation of type I fibers? The *FOXO1* transgene is expressed in muscles rich in both type I and type II fibers. How does it cause the selective reduction of gene expression in type I fibers but not in type II fibers? It is possible that FOXO1 suppresses the function of a factor(s) that is preferentially expressed in type I fibers and therefore activates gene expression only in type I fibers. One candidate for such a factor is PGC-1α, which is known to be preferentially expressed in type I fibers and enhances type I fiber gene expression (22). As the FOXO1 protein can interact with the PGC-1α protein (43), FOXO1 may affect certain functions of PGC-1α. FOXO1 may inhibit PGC-1α function via its binding to PGC-1α. FOXO1 itself is a transcription factor. In addition, several reports (27–30) have shown that FOXO1 acts as a corepressor of nuclear receptors, whereas PGC-1α can activate many nuclear receptors (21, 63). Although to our knowledge nuclear receptors have not been shown to be involved in type I fiber-specific gene expression, a certain nuclear receptor(s) and transcription factor(s), which can interact with both FOXO1 and PGC-1α, may be involved in a process positively and negatively regulated by PGC-1α and FOXO1, respectively. Further studies are required to examine this possibility. Besides, although PGC-1α stimulates the differentiation of type I fibers, in FOXO1 mice, gene expression was reduced in type I fibers but was not affected in type II fibers. Thus, fiber differentiation (switching) from type I to type II is not likely to occur in FOXO1 mice, and FOXO1 appears not to be involved in fiber differentiation.

Calcineurin (14, 17) and CaMK (15), downstream molecules of calcium signaling (13), the transcription factors Mef2c (14–16, 18) and NFAT (14, 15, 17), as well as the nuclear receptor coactivator PGC-1α (22) are known to promote type I fiber differentiation and type I fiber gene expression. In skeletal muscle of FOXO1 mice, mRNA levels of Mef2c and CaMK are significantly decreased (Fig. 2*A*). FOXO1 may reduce gene expression in type I fiber by suppressing gene expression of Mef2c and CaMK.

FOXO1 mice showed a clear phenotype related to the function of skeletal muscle. Specifically, spontaneous locomotor activity was lower in FOXO1 mice than in control mice (Fig. 3*B*). In addition, FOXO1 mice had impaired oral glucose tolerance and impaired insulin-mediated glucose-lowering effects (Fig. 3, *C* and *D*). Elderly humans have been reported to show

a progressive loss of muscle fibers associated with diabetes, obesity, and decreased physical activity (sarcopenia). Overexpression of IGF-1 in skeletal muscle prevents the age-related decline in muscle mass (11, 57). As described above, the reduced skeletal muscle mass in FOXO1 mice may be caused by the suppression of IGF signaling during skeletal muscle formation, and FOXO1 may therefore be involved in age-related sarcopenia in humans. FOXO1 mice may be valuable as a model for human diseases related to loss of muscle fibers. Further analysis of the molecular mechanisms of FOXO1 action in skeletal muscle is important from a clinical as well as a sports science perspective.

Acknowledgments—We thank H. Meguro for technical assistance, Dr. S. Machida (University of Missouri, Columbia) for valuable comments, and Dr. H. A. Popiel for proofreading.

REFERENCES

1. Zurlo, F., Larson, K., Bogardus, C., and Ravussin, E. (1990) *J. Clin. Investig.* **86,** 1423–1427
2. Berchtold, M. W., Brinkmeier, H., and Muntener, M. (2000) *Physiol. Rev.* **80,** 1215–1265
3. Proctor, D., Balagopal, P., and Nair, K. (1998) *J. Nutr.* **128,** S351–S355
4. Fitts, R., Riley, D., and Widrick, J. (2001) *J. Exp. Biol.* **204,** 3201–3208
5. Hickey, M. S., Carey, J. O., Azevedo, J. L., Houmard, J. A., Pories, W. J., Israel, R. G., and Dohm, G. L. (1995) *Am. J. Physiol.* **268,** E453–E457
6. Gaster, M., Staehr, P., Beck-Nielsen, H., Schroder, H. D., and Handberg, A. (2001) *Diabetes* **50,** 1324–1329
7. Tanner, C. J., Barakat, H. A., Dohm, G. L., Pories, W. J., MacDonald, K. G., Cunningham, P. R., Swanson, M. S., and Houmard, J. A. (2002) *Am. J. Physiol.* **282,** E1191–E1196
8. Frost, R. A., and Lang, C. H. (2003) *Minerva Endocrinol.* **28,** 53–73
9. DeVol, D., Rotwein, P., Sadow, J., Novakofski, J., and Bechtel, P. (1990) *Am. J. Physiol.* **259,** E89–E95
10. Zdanowicz, M., Moyse, J., Wingertzahn, M., O'Connor, M., Teichberg, S., and Slonim, A. (1995) *Endocrinology* **136,** 4880–4886
11. Barton-Davis, E. R., Shoturma, D. I., Musaro, A., Rosenthal, N., and Sweeney, H. L. (1998) *Proc. Natl. Acad. Sci. U. S. A.* **95,** 15603–15607
12. Florini, J., Ewton, D., and Coolican, S. (1996) *Endocr. Rev.* **17,** 481–517
13. Stull, J. T. (2001) *J. Biol. Chem.* **276,** 2311–2312
14. Chin, E. R., Olson, E. N., Richardson, J. A., Yang, Q., Humphries, C., Shelton, J. M., Wu, H., Zhu, W., Bassel-Duby, R., and Williams, R. S. (1998) *Genes Dev.* **12,** 2499–2509
15. Wu, H., Naya, F. J., McKinsey, T. A., Mercer, B., Shelton, J. M., Chin, E. R., Simard, A. R., Michel, R. N., Bassel-Duby, R., Olson, E. N., and Williams, R. S. (2000) *EMBO J.* **19,** 1963–1973
16. Yan, Z., Serrano, A. L., Schiaffino, S., Bassel-Duby, R., and Williams, R. S. (2001) *J. Biol. Chem.* **276,** 17361–17366
17. Chakkalakal, J. V., Stocksley, M. A., Harrison, M. A., Angus, L. M., Deschenes-Furry, J., St-Pierre, S., Megeney, L. A., Chin, E. R., Michel, R. N., and Jasmin, B. J. (2003) *Proc. Natl. Acad. Sci. U. S. A.* **100,** 7791–7796
18. Karasseva, N., Tsika, G., Ji, J., Zhang, A., Mao, X., and Tsika, R. (2003) *Mol. Cell. Biol.* **23,** 5143–5164
19. Kamei, Y., Xu, L., Heinzel, T., Torchia, J., Kurokawa, R., Gloss, B., Lin, S. C., Heyman, R. A., Rose, D. W., Glass, C. K., and Rosenfeld, M. G. (1996) *Cell* **85,** 403–414
20. Glass, C. K., Rose, D. W., and Rosenfeld, M. G. (1997) *Curr. Opin. Cell Biol.* **9,** 222–232
21. Puigserver, P., Wu, Z., Park, C. W., Graves, R., Wright, M., and Spiegelman, B. M. (1998) *Cell* **92,** 829–839
22. Lin, J., Wu, H., Tarr, P. T., Zhang, C. Y., Wu, Z., Boss, O., Michael, L. F., Puigserver, P., Isotani, E., Olson, E. N., *et al.* (2002) *Nature* **418,** 797–801
23. Miura, S., Kai, Y., Ono, M., and Ezaki, O. (2003) *J. Biol. Chem.* **278,** 31385–31390
24. Anderson, M. J., Viars, C. S., Czekay, S., Cavenee, W. K., and Arden, K. C. (1998) *Genomics* **47,** 187–199
25. Kaestner, K. H., Knochel, W., and Martinez, D. E. (2000) *Genes Dev.* **14,** 142–146
26. Galili, N., Davis, R. J., Fredericks, W. J., Mukhopadhyay, S., Rauscher, F. J., 3rd, Emanuel, B. S., Rovera, G., and Barr, F. G. (1993) *Nat. Genet.* **5,** 230–235
27. Schuur, E. R., Loktev, A. V., Sharma, M., Sun, Z., Roth, R. A., and Weigel, R. J. (2001) *J. Biol. Chem.* **276,** 33554–33560
28. Zhao, H. H., Herrera, R. E., Coronado-Heinsohn, E., Yang, M. C., Ludes-Meyers, J. H., Seybold-Tilson, K. J., Nawaz, Z., Yee, D., Barr, F. G., Diab, S. G., Brown, P. H., Fuqua, S. A. W., and Osborne, C. K. (2001) *J. Biol. Chem.* **276,** 27907–27912
29. Dowell, P., Otto, T. C., Adi, S., and Lane, M. D. (2003) *J. Biol. Chem.* **278,** 45485–45491
30. Hirota, K., Daitoku, H., Matsuzaki, H., Araya, N., Yamagata, K., Asada, S., Sugaya, T., and Fukamizu, A. (2003) *J. Biol. Chem.* **278,** 13056–13060
31. Ayala, J. E., Streeper, R. S., Desgrosellier, J. S., Durham, S. K., Suwanichkul, A., Svitek, C. A., Goldman, J. K., Barr, F. G., Powell, D. R., and O'Brien, R. M. (1999) *Diabetes* **48,** 1885–1889
32. Barthel, A., Schmoll, D., Kruger, K. D., Bahrenberg, G., Walther, R., Roth, R. A., and Joost, H. G. (2001) *Biochem. Biophys. Res. Commun.* **285,** 897–902
33. Nakae, J., Kitamura, T., Silver, D. L., and Accili, D. (2001) *J. Clin. Investig.* **108,** 1359–1367
34. Nadal, A., Marrero, P. F., and Haro, D. (2002) *Biochem. J.* **366,** 289–297
35. Dijkers, P. F., Medema, R. H., Pals, C., Banerji, L., Thomas, N. S. B., Lam, E. W. F., Burgering, B. M. T., Raaijmakers, J. A. M., Lammers, J. W. J., Koenderman, L., and Coffer, P. J. (2000) *Mol. Cell. Biol.* **20,** 9138–9148
36. Medema, R. H., Kops, G. J. P. L., Bos, J. L., and Burgering, B. M. T. (2000) *Nature* **404,** 782–787
37. Brunet, A., Bonni, A., Zigmond, M. J., Lin, M. Z., Juo, P., Hu, L. S., Anderson, M. J., Arden, K. C., Blenis, J., and Greenberg, M. E. (1999) *Cell* **96,** 857–868
38. Kops, G. J. P. L., Dansen, T. B., Polderman, P. E., Saarloos, I., Wirtz, K. W. A., Coffer, P. J., Huang, T. T., Bos, J. L., Medema, R. H., and Burgering, B. M. T. (2002) *Nature* **419,** 316–321
39. Nakae, J., Kitamura, T., Kitamura, Y., Biggs, W. H., III, Arden, K. C., and Accili, D. (2003) *Dev. Cell* **4,** 119–129
40. Bois, P. R. J., and Grosveld, G. C. (2003) *EMBO J.* **22,** 1147–1157
41. Nakae, J., Biggs, W. H., III, Kitamura, T., Cavenee, W. K., Wright, C. V., Arden, K. C., and Accili, D. (2002) *Nat. Genet.* **32,** 245–253
42. Kamei, Y., Mizukami, J., Miura, S., Suzuki, M., Takahashi, N., Kawada, T., Taniguchi, T., and Ezaki, O. (2003) *FEBS Lett.* **536,** 232–236
43. Puigserver, P., Rhee, J., Donovan, J., Walkey, C. J., Yoon, J. C., Oriente, F., Kitamura, Y., Altomonte, J., Dong, H., Accili, D., and Spiegelman, B. M. (2003) *Nature* **423,** 550–555
44. Ogg, S., Paradis, S., Gottlieb, S., Patterson, G. I., Lee, L., Tissenbaum, H. A., and Ruvkun, G. (1997) *Nature* **389,** 994–999
45. Brennan, K. J., and Hardeman, E. C. (1993) *J. Biol. Chem.* **268,** 719–725
46. Nagy, T. R., and Clair, A. L. (2000) *Obes. Res.* **8,** 392–398
47. Hahn, C. G., and Covault, J. (1990) *Anal. Biochem.* **190,** 193–197
48. Ogilvie, R. W., and Feeback, D. L. (1990) *Stain Technol.* **65,** 231–241
49. Takahashi, M., Tsuboyama-Kasaoka, N., Nakatani, T., Ishii, M., Tsutsumi, S., Aburatani, H., and Ezaki, O. (2002) *Am. J. Physiol.* **282,** G338–G348
50. Adams, M. D., Kerlavage, A. R., Fleischmann, R. D., Fuldner, R. A., Bult, C. J., Lee, N. H., Kirkness, E. F., Weinstock, K. G., Gocayne, J. D., White, O., *et al.* (1995) *Nature* **377,** 3–174
51. Furukawa-Hibi, Y., Yoshida-Araki, K., Ohta, T., Ikeda, K., and Motoyama, N. (2002) *J. Biol. Chem.* **277,** 26729–26732
52. Tran, H., Brunet, A., Grenier, J. M., Datta, S. R., Fornace, A. J., Jr., DiStefano, P. S., Chiang, L. W., and Greenberg, M. E. (2002) *Science* **296,** 530–534
53. Furuyama, T., Kitayama, K., Yamashita, H., and Mori, N. (2003) *Biochem. J.* **375,** 365–371
54. Garry, D. J., Ordway, G. A., Lorenz, J. N., Radford, N. B., Chin, E. R., Grange, R. W., Bassel-Duby, R., and Williams, R. S. (1998) *Nature* **395,** 905–908
55. Lecker, S., Jagoe, R., Gilbert, A., Gomes, M., Baracos, V., Bailey, J., Price, S., Mitch, W., and Goldberg, A. (2004) *FASEB J.* **18,** 39–51
56. Ezaki, O. (1997) *Biochem. Biophys. Res. Commun.* **241,** 1–6
57. Chakravarthy, M., Davis, B., and Booth, F. (2000) *J. Appl. Physiol.* **89,** 1365–1379
58. Machida, S., Spangenburg, E., and Booth, F. (2003) *J. Cell. Physiol.* **196,** 523–531
59. Yamanouchi, K., Soeta, C., Suzuki, S., Hasegawa, T., Naito, K., and Tojo, H. (2000) *J. Vet. Med. Sci.* **62,** 1213–1216
60. Sandri, M., Sandri, C., Gilbert, A., Skurk, C., Calabria, E., Picard, A., Walsh, K., Schiaffino, S., Lecker, S., and Goldberg, A. (2004) *Cell* **117,** 399–412
61. Stitt, T., Drujan, D., Clarke, B., Panaro, F., Timofeyva, Y., Kline, W., Gonzalez, M., Yancopoulos, G., and Glass, D. (2004) *Mol. Cell* **14,** 395–403
62. Schneider, M., Wolf, E., Hoeflich, A., and Lahm, H. (2002) *J. Endocrinol.* **172,** 423–440
63. Kamei, Y., Ohizumi, H., Fujitani, Y., Nemoto, T., Tanaka, T., Takahashi, N., Kawada, T., Miyoshi, M., Ezaki, O., and Kakizuka, A. (2003) *Proc. Natl. Acad. Sci. U. S. A.* **100,** 12378–12383

Available online at www.sciencedirect.com
SCIENCE DIRECT®
General and Comparative Endocrinology 138 (2004) 281–286
GENERAL AND COMPARATIVE ENDOCRINOLOGY
www.elsevier.com/locate/ygcen

Communication in Genomics and Proteomics

Sequence analysis of cDNA encoding follicle-stimulating hormone and luteinizing hormone β-subunits in the Mastomys (*Praomys coucha*)

Kaoru Takano, Minako Koura, Yoko Noguchi, Yoshie Yamamoto, Kozue Uchio-Yamada, Junichiro Matsuda, Osamu Suzuki*

Department of Veterinary Science, National Institute of Infectious Diseases, 1-23-1 Toyama, Shinjuku-ku, Tokyo 162-8640, Japan

Received 26 March 2004; revised 19 June 2004; accepted 24 June 2004
Available online 18 August 2004

Abstract

To examine the molecular basis of efficient superovulation in the Mastomys (*Praomys coucha*), the cDNA sequences of the follicle-stimulating hormone (FSH) and luteinizing hormone (LH) β-subunits were determined and compared with those of other mammals. FSHβ and LHβ cDNAs were 1606 and 513 bp long, respectively, from the 5′-ends to the putative polyA sites. The deduced sequences of the FSHβ and LHβ precursor proteins were 130 and 141 amino acids in length, respectively. The amino acid sequences of both mastomys hormone subunits showed overall similarity to those of other rodents. In particular, the N-terminus of the FSHβ precursor protein is of the MM-type, like those of mice and rats, which suggests that the MM-type is characteristic of the subfamily *Murinae*. As we reported earlier for the Mongolian gerbil, the use of hCG for superovulation of mastomys might need to be re-evaluated, due to the low homology between hCG and rodent LH sequences.

Keywords: Mastomys; FSHβ; LHβ; cDNA; Phylogeny

1. Introduction

The mastomys (multimammate mouse, *Praomys coucha*) is an African rodent that is a well-known reservoir of serious diseases, such as *Yersinia pestis*, the rickettsia that causes bubonic plague (Dippenaar et al., 1993). It is used as a laboratory animal for studies of virology, oncology, and reproductive biology (Solleveld, 1987). For instance, *mastomys* are used to study prostate endocrinology, since both males and females have functional prostates (Ohta et al., 1994). Although there has been some research on reproduction technology in mastomys (Nohara et al., 1998; Ogonuki et al., 2003), it is quite difficult to apply standard embryo manipulation techniques, such as transgenic technologies or cryopreservation of embryos and gametes, to mastomys. Many embryos and oocytes are required to establish these techniques, necessitating the induction of superovulation. In mastomys, the combination of equine chorionic gonadotropin (eCG) plus human chorionic gonadotropin (hCG) is effective for superovulation, but a problem arises in that treated females rarely have fertile matings, perhaps due to a perturbation of estrous behavior by the exogenous hormones (Ogura et al., 1997). More information is needed to permit a careful selection of appropriate gonadotropins that will be practical and functional for superovulation in this animal.

This paper describes the cDNA sequences of the follicle-stimulating hormone (FSH) and luteinizing hormone (LH) β-subunits in order to develop a molecular

* Corresponding author. Fax: +81-3-5285-1179.
E-mail address: osuzuki@nih.go.jp (O. Suzuki).

0016-6480/$ - see front matter © 2004 Elsevier Inc. All rights reserved.
doi:10.1016/j.ygcen.2004.06.009

basis for efficient superovulation in the mastomys. Phylogenetic analyses of the deduced protein sequences were also performed. The possibility of using this sequence information as a criterion for selecting gonadotropins for superovulation in the mastomys is discussed.

2. Materials and methods

2.1. RNA extraction, RT-PCR, and sequencing

The full sequences of FSHβ and LHβ were determined using a combination of 5′- and 3′-rapid amplification of cDNA ends (RACE) using a SMART RACE cDNA amplification kit (BD Biosciences Clontech, Palo Alto, CA), followed by direct sequencing of the RACE products. In brief, two cDNA libraries for RACE reactions were prepared from total RNA extracted from pituitaries of male mastomys of the MCC strain. RACE reactions were performed using these libraries, a DNA polymerase mixture (HotStarTaq Master Mix, Qiagen GmbH, Hilden, Germany), anchor primers (universal primer mix included in the kit), and gene-specific primers. Amplification was completed using a Hybaid PCR Express thermal cycler (Thermo Bioanalysis Japan KK, Tokyo, Japan) under the following thermal conditions: one cycle at 94 °C for 15 min (denaturation and enzyme activation), and 40 cycles of 94 °C for 2 s and 68 °C for 5 min.

To determine the FSHβ sequence, nested PCR amplifications for primer walking were carried out with the primary PCR products (diluted 1:50), a DNA polymerase mixture, nested adaptor primers (included in the kit), and gene-specific primers under the following thermal conditions: one cycle at 94 °C for 15 min; 40 cycles of 94 °C for 10 s, 60 °C for 10 s, and 72 °C for 1 min; and one cycle of 72 °C for 10 min. The positions of the gene-specific primers used in the RACE reactions are shown in Fig. 1. For the FSHβ cDNA sequence, 5′-RACE was first conducted with primer 5Fp (TTC CTT CAT TTC ACT GAA GGA GCA GTA). Then primer walking was performed in 3′-RACE reactions with a total of four primers: 3Fp1 (GGA CCC AGC TCG ACC CAA TAC CCA GAA), 3Fp2 (CGC CAC TCA TCC CTC TAT CCA GAC TGT TG), 3Fp3 (GCA CGA CCA TCT GCC TTT TTA GAG CCA TC), and 3Fp4 (TTG CAT GCA GGG AGG GAA GGT TTT GAA). For the LHβ sequence, 3′-RACE was first conducted with primer 3Lp (GGC TGC TGC TGA GCC CAA GTG TGG TGT), followed by 5′-RACE with primer 5Lp (TGA GTC CTG GGA CCC CCA CAG TCA GAG). Both 5Fp and 3Lp were designed from mouse sequences (NP_032071and NM_008497 from GenBank for FSHβ and LHβ, respectively) using Primer3 software (Rozen and Skaletsky, 1998). The other primers were then designed using Primer3 with the newly determined, partial sequences. The obtained RACE products were gel-purified and sequenced directly using a DYEnamic ET Terminator Cycle Sequencing Kit (Amersham Biosciences, Piscataway, NJ) with a DNA sequencer (RISA384, Shimadzu Biotech, Kyoto, Japan). Full sequences were obtained by combining the overlapping sequences of the 5′- and 3′-RACE products. The 5′- and 3′-ends of the cDNA sequences were determined by the appearance of SMART II Oligo- and putative polyA-sequences, respectively, in the sequenced RACE products.

2.2. Molecular phylogenetic analysis

Additional mammalian FSHβ and LHβ sequences were retrieved from GenBank as follows (Accession Nos. are shown in parentheses): mouse (NP_032071and NM_008497), rat (P18427 and J00749), pig (P01228 and D00579), cattle (NP_776485 and M10077), sheep (P01227 and X52488), horse (P01226 and S41704), human (P01225 and NM_000894), Mongolian gerbils (AY376457 and AY369077), and Djungarian hamsters (*Phodopus sungorus*; AF106914 and AF106915). The amino acid sequence of hCG was also retrieved from GenBank (J00117). The amino acid sequences of these species, including the mastomys, were aligned using Clustal X, version 1.81 (Thompson et al., 1997). Neighbor-joining (NJ) trees containing the FSHβ and LHβ protein sequences of nine species (the Djungarian hamster was omitted because both AF106914 and AF106915 were partial sequences) were constructed using MEGA, version 2.1 (Kumar et al., 2001), based on the number of amino acid substitutions with 5000 bootstrap iterations.

3. Results and discussion

The full-length FSHβ and LHβ cDNA sequences are shown in Fig. 1. Both sequences have been deposited in GenBank with Accession Nos. AY458603 and AY353073, respectively. The FSHβ and LHβ cDNAs were 1606 and 513 bp long, respectively, from the 5′-end to putative polyA sites. Both sequences contained putative polyA signal sequences (AATAAA), starting at positions 1588 and 494, respectively, for FSHβ and LHβ. The deduced sequences of the FSHβ and LHβ precursor proteins were 130 and 141 amino acids in length, respectively. Both amino acid sequences contained the

Fig. 1. Sequences of FSHβ (A) and LHβ (B) subunit cDNAs. The deduced amino acid sequences of both sequences are shown in bold face. Putative polyadenylation signal sequences are boxed and putative polyadenylation sites are indicated by asterisks (*). Arrows indicate primer positions (5Fp, 3Fp1, 3Fp2, 3Fp3, 3Fp4, 5Lp, and 3Lp).

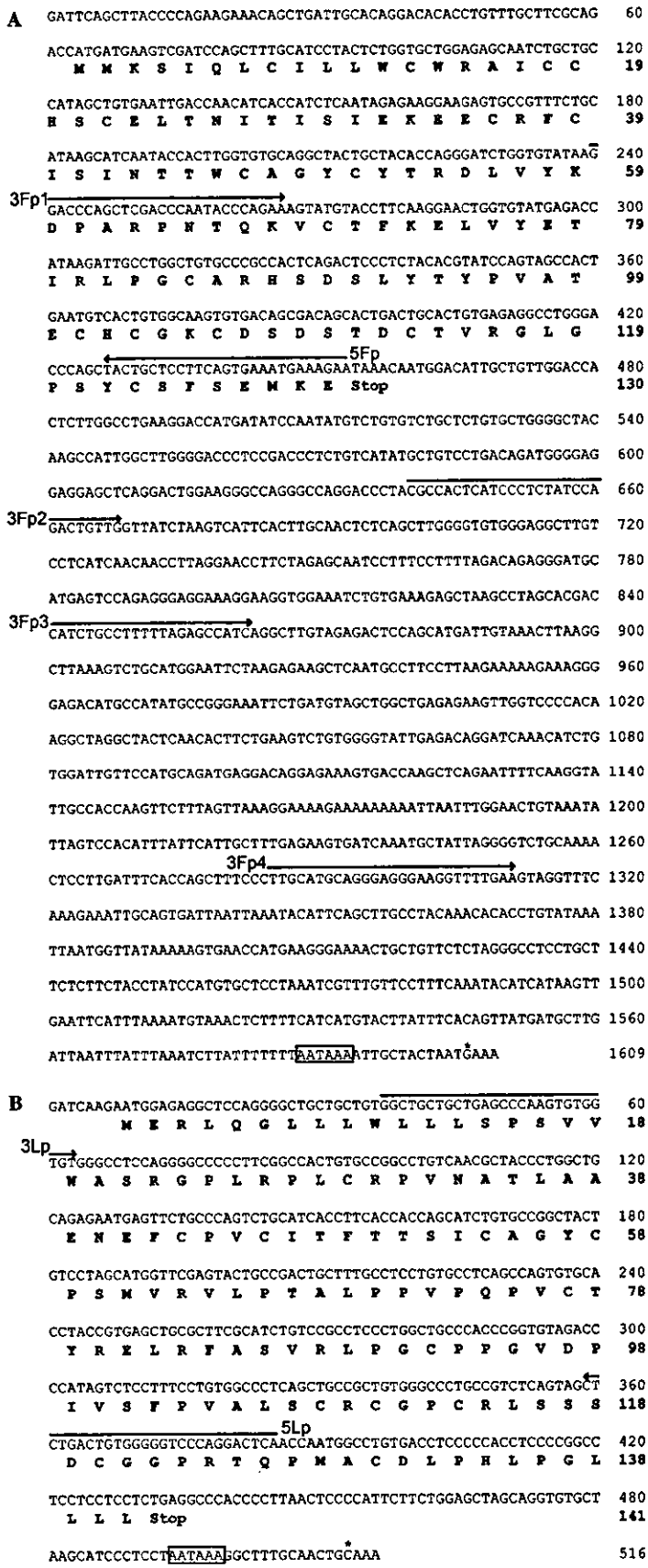
A
3Fp1
5Fp
3Fp2
3Fp3
3Fp4
B
3Lp
5Lp

unique β-subunit sequence CAGY, which is thought to be a key structure for binding to common α-subunits (Gharib et al., 1990). The positions of half-cysteine residues and putative N-glycosylation sites were well conserved in comparison with those of other mammals. The mastomys FSHβ cDNA shares the common feature of a long 3′-UTR with other mammals.

The alignments of the amino acid sequences indicate the overall similarity of both mastomys β-subunits to those of other rodents (Fig. 2). The phylogenetic analysis of each protein (Fig. 3) also supports the similarity of these two hormones among rodents, especially within *Murinae* (mouse, rat, and mastomys). As we reported earlier (Koura et al., 2004), there are two variations of

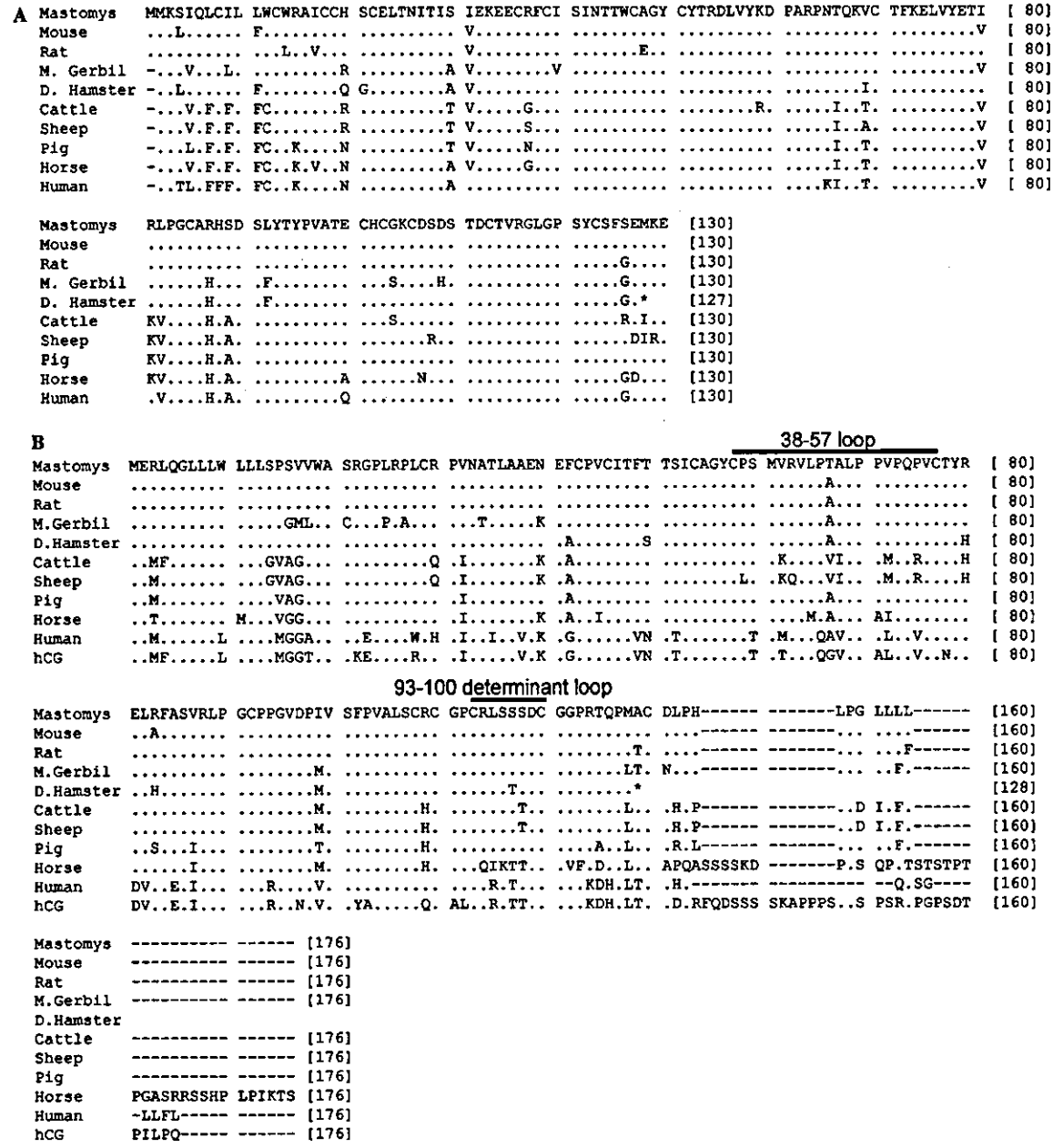

Fig. 2. Alignments of the amino acid sequences of the FSHβ (A) and LHβ (B) subunits in 10 mammalian species. The mastomys, mouse, and rat belong to the subfamily *Murinae*, the Mongolian gerbil (M. Gerbil) to *Gerbillinae*, and the Djungarian hamster (D. Hamster) to *Cricetinae*. hCG is also included in panel B. A dot indicates an amino acid residue identical to the corresponding site in the mastomys sequence (top row). Dashes in the sequences indicate gaps inserted by Clustal X software. Asterisks (*) indicate the ends of currently available, partial sequences for the Djungarian hamster. Note that two regions of the rodent LHβ sequences shown in panel B (the 38–57 and 93–100 determinant loops; the position numbers of the amino acids correspond to the mature proteins, not the precursor protein), which are responsible for receptor binding and activation, have lower homologies with hCGβ than do the LHβs of domestic animals.

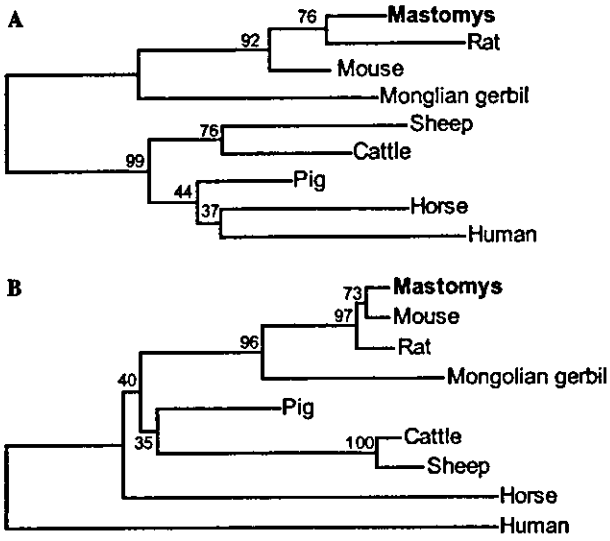

Fig. 3. Phylogenetic trees constructed from the inferred amino acid sequences of the FSHβ (A) and LHβ (B) subunits of nine mammalian species. The figures at the nodes represent bootstrap values based on 5000 iterations.

the amino-terminus of the FSHβ precursor protein in laboratory rodents: MM- and M-types. The former type seems characteristic of animals belonging to the subfamily *Murinae*, since mastomys, mice, and rats all have this type of FSHβ precursor protein. In contrast, Djungarian hamsters (subfamily *Cricetinae*) and Mongolian gerbils (subfamily *Gerbillinae*) have the latter type of amino-terminus (Bernard et al., 2000; Koura et al., 2004), suggesting their phylogenetic distance from *Murinae*. So far, FSHβ and LHβ cDNA sequences have been reported for only a few rodent species. More research is needed to define more precisely the rodent-specific features of these proteins.

The efficacy and species-spectrum of a conventional regimen for induction of ovulation using a combination of eCG and hCG should be re-evaluated. Ovulation in mastomys can be induced by the combination of eCG and hCG injections, as is used for superovulation of mice and rats. The similarity of the response in mastomys, rats, and mice may be due in part to the similarity between the β-subunits of their gonadotropins. As discussed previously for the Mongolian gerbil (Koura et al., 2004), however, hCG should ideally be replaced with native LH, or an LH with greater similarity, since the species-specificities of LHs are reportedly higher than those of FSHs (Ishii and Kubokawa, 1984). A considerable number of antral follicles often remain in the ovaries of mastomys after they have received both eCG and hCG (unpublished observation). The low incidence of fertile matings (Ogura et al., 1997) also suggests that use of hCG as an ovulation inducer is inappropriate in mastomys. The amino acid sequences of the β-subunits of human origin (LHβ and hCGβ) show low homology to those of other luteinizing hormones (Fig. 2). In particular, two regions of rodent LHβ (the 38–57 and 93–100 determinant loops shown in Fig. 2B), which are thought to be responsible for receptor binding and activation (reviewed by Bousfield et al., 1994), are less homologous to the corresponding regions in hCGβ than are the LHβ sequences of domestic animals. In addition, the common α-subunit of mastomys gonadotropins and thyrotropin is less similar to that of humans than are those of other mammals (Suzuki et al., 2002). These low homologies between mastomys and human gonadotropins suggest that better inducers of ovulation in mastomys should be sought, rather than relying on human gonadotropins. One possibility is to invoke a surge in endogenous LH by promoting follicle development by repeated administration of FSH, instead of eCG. FSH would be a better choice for this application than eCG, because the shorter half-life of FSH makes it less likely to perturb endocrine systems. Using this strategy, we successfully induced superovulation in guinea pigs by repeated administration of human menopausal gonadotropins (hMG), without the use of any LH equivalents, such as hCG (Suzuki et al., 2003). In that case, we used human-derived FSH because of the high homology between guinea pig and human FSH-receptor sequences. Although the sequence of the mastomys FSH-receptor has not yet been reported, repeated administration of hMG might also work to induce superovulation in mastomys since species differences in FSHβ sequences are less than those of LHβ. The affinity and efficacy of native hormones in various rodents should be evaluated and compared with those of hCG by producing recombinant hormones.

In summary, we determined the cDNA sequences of the FSH and LH β-subunits of the mastomys. This information should provide a molecular basis for understanding hormonal control of ovulation, as well as improving superovulation technologies in the mastomys.

References

Bernard, D.J., Merzlyak, I.Y., Horton, T.H., Turek, F.W., 2000. Differential regulation of pituitary gonadotropin subunit messenger ribonucleic acid levels in photostimulated Siberian hamsters. Biol. Reprod. 62, 155–161.

Bousfield, G.R., Perry, W.M., Ward, D.N., 1994. Gonadotropins. In: Knobil, E., Neill, J.D. (Eds.), The Physiology of Reproduction. Raven Press Ltd, New York, pp. 1749–1792.

Dippenaar, N.J., Swanepoel, P., Gordon, D.H., 1993. Diagnostic morphometrics of two medically important southern African rodents, *Mastomys natalensis* and *M. coucha* (Rodentia: Muridae). South Afr. J. Sci. 89, 300–303.

Gharib, S.D., Wierman, M.E., Shupnik, M.A., Chin, W.W., 1990. Molecular biology of the pituitary gonadotropins. Endocr. Rev. 11, 177–199.

Ishii, S., Kubokawa, K., 1984. Avian gonadotropin receptors: a comparative view. J. Exp. Zool. 232, 431–434.

Koura, M., Handa, H., Noguchi, Y., Takano, K., Yamamoto, Y., Matsuda, J., Suzuki, O., 2004. Sequence analysis of cDNA encoding follicle-stimulating hormone and luteinizing hormone β-subunits in the Mongolian gerbil (*Meriones unguiculatus*). Gen. Comp. Endocrinol. 136, 406–410.

Kumar, S., Tamura, K., Jakobsen, I.B., Nei, M., 2001. MEGA2: molecular evolutionary genetics analysis software. Bioinformatics 17, 1244–1245.

Nohara, M., Hirayama, T., Ogura, A., Hiroi, M., Araki, Y., 1998. Partial characterization of the gametes and development of a successful in vitro fertilization procedure in the mastomys (*Praomys coucha*): a new species for reproductive biology research. Biol. Reprod. 58, 226–233.

Ogonuki, N., Mochida, K., Inoue, K., Matsuda, J., Yamamoto, Y., Takano, K., Ogura, A., 2003. Fertilization of oocytes and birth of normal pups following intracytoplasmic injection with spermatids in mastomys (*Praomys coucha*). Biol. Reprod. 68, 1821–1827.

Ogura, A., Matsuda, J., Mochida, K., Suzuki, O., Takimoto, K., Nakayama, K., Naiki, M., 1997. Preimplantation embryo development in Mastomys (*Praomys coucha*) in vivo and in vitro. J. Reprod. Dev. 43, 65–71.

Ohta, A., Mizoguchi, Y., Kano, Y., 1994. Effects of TAP-144-SR administration on the prostates of male and female mastomys. J. Reprod. Dev. 40, 329–335.

Rozen, S., Skaletsky, H.J., 1998. Primer3. Code Available from <http://www-genome.wi.mit.edu/genome_software/other/primer3.html>.

Solleveld, H.A., 1987. The multimammate mouse. In: Poole, T.B. (Ed.), The UFAW Handbook on the Care and Management of Laboratory Animals, sixth ed. Longman Scientific & Technical, Harlow, pp. 346–359.

Suzuki, O., Koura, M., Noguchi, Y., Takano, K., Yamamoto, Y., Matsuda, J., 2003. Optimization of superovulation induction by human menopausal gonadotropin in guinea pigs based on follicular waves and FSH-receptor homologies. Mol. Reprod. Dev. 64, 219–225.

Suzuki, O., Mochida, K., Yamamoto, Y., Noguchi, Y., Takano, K., Matsuda, J., Ogura, A., 2002. Comparison of glycoprotein hormone α-subunits of laboratory animals. Mol. Reprod. Dev. 62, 335–342.

Thompson, J.D., Gibson, T.J., Plewniak, F., Jeanmougin, F., Higgins, D.G., 1997. The CLUSTAL_X windows interface: flexible strategies for multiple sequence alignment aided by quality analysis tools. Nucleic Acids Res. 25, 4876–4882.